common mechanism for organogenesis and pathogenesis of human diseases.

ACKNOWLEDGMENTS

We thank Dr. Mark Knepper (National Heart, Lung, and Blood Institute) for the aquaporin-2 antibody.

GRANTS

This work was supported by Grants-in-Aid for Scientific Research from the Ministry of Education, Culture, Sports, Science, and Technology, Japan, Grants-in-Aid for Scientific Research from the Ministry of Health, Labour, and Welfare of Japan, a Research Grant from Uehara Memorial Foundation, the University of Texas Southwestern O'Brien Kidney Research Core Center (National Institute of Diabetes and Digestive and Kidney Diseases Grant P30DK-079328), and a Basil O'Connor Research Grant from the March of Dimes Birth Defects Foundation.

REFERENCES

1. **Barnes PJ.** New concepts in chronic obstructive pulmonary disease. *Annu Rev Med* 54: 113–129, 2003.
2. **Benezra R.** Polycystins: inhibiting the inhibitors. *Nat Cell Biol* 7: 1064–1065, 2005.
3. **Bisceglia M, Galliani CA, Senger C, Stallone C, Sessa A.** Renal cystic diseases: a review. *Adv Anat Pathol* 13: 26–56, 2006.
4. **Chen Q, Takahashi S, Zhong S, Hosoda C, Zheng HY, Ogushi T, Fujimura T, Ohta N, Tanoue A, Tsujimoto G, Kitamura T.** Function of the lower urinary tract in mice lacking alpha1d-adrenoceptor. *J Urol* 174: 370–374, 2005.
5. **Cui CB, Cooper LF, Yang X, Karsenty G, Aukhil I.** Transcriptional coactivation of bone-specific transcription factor Cbfa1 by TAZ. *Mol Cell Biol* 23: 1004–1013, 2003.
6. **D'Angelo A, Mioni G, Ossi E, Lupo A, Valvo E, Maschio G.** Alterations in renal tubular sodium and water transport in polycystic kidney disease. *Clin Nephrol* 3: 99–105, 1975.
7. **Deen PMT.** Mouse models for congenital nephrogenic diabetes insipidus: what can we learn from them? *Nephrol Dial Transplant* 22: 1023–1026, 2007.
8. **Dressler GR.** Tubulogenesis in the developing mammalian kidney. *Trends Cell Biol* 12: 390–395, 2002.
9. **Glasser SW, Detmer EA, Ikegami M, Na CL, Stahlman MT, Whitsett JA.** Pneumonitis and emphysema in sp-C gene targeted mice. *J Biol Chem* 278: 14291–14298, 2003.
10. **Guay-Woodford LM.** Murine models of polycystic kidney disease: molecular and therapeutic insights. *Am J Physiol Renal Physiol* 285: F1034–F1049, 2003.
11. **Gusmano R, Caridi G, Marini M, Perfumo F, Ghiggeri GM, Piaggio G, Ceccherini I, Seri M.** Glomerulocystic kidney disease in a family. *Nephrol Dial Transplant* 17: 813–818, 2002.
12. **Hogg JC.** Pathophysiology of airflow limitation in chronic obstructive pulmonary disease. *Lancet* 364: 709–721, 2004.
13. **Hong JH, Hwang ES, McManus MT, Amsterdam A, Tian Y, Kalmukova R, Mueller E, Benjamin T, Spiegelman BM, Sharp PA, Hopkins N, Yaffe MB.** TAZ, a transcriptional modulator of mesenchymal stem cell differentiation. *Science* 309: 1074–1078, 2005.
14. **Hong JH, Yaffe MB.** TAZ: a β-catenin-like molecule that regulates mesenchymal stem cell differentiation. *Cell Cycle* 5: 176–179, 2006.
15. **Horie S.** ADPKD: molecular characterization and quest for treatment. *Clin Exp Nephrol* 9: 282–291, 2005.
16. **Hossain Z, Ali SM, Ko HL, Xu J, Ng CP, Guo K, Qi Z, Ponniah S, Hong W, Hunziker W.** Glomerulocystic kidney disease in mice with a targeted inactivation of Wwtr1. *Proc Natl Acad Sci USA* 104:1631–1636, 2007.
17. **Hu MC, Rosenblum ND.** Genetic regulation of branching morphogenesis: lessons learned from loss-of-function phenotypes. *Pediatr Res* 54: 433–438, 2003.
18. **Kanai F, Marignani PA, Sarbassova D, Yagi R, Hall RA, Donowitz M, Hisaminato A, Fujiwara T, Ito Y, Cantley LC, Yaffe MB.** TAZ: a novel transcriptional co-activator regulated by interactions with 14-3-3 and PDZ domain proteins. *EMBO J* 19: 6778–6791, 2000.
19. **Li X, Luo Y, Starremans PG, McNamara CA, Pei Y, Zhou J.** Polycystin-1 and polycystin-2 regulate the cell cycle through the helix-loop-helix inhibitor Id2. *Nat Cell Biol* 7: 1102–1112, 2005.
20. **Lu W, Peissel B, Babakhanlou H, Pavlova A, Geng L, Fan X, Larson C, Brent G, Zhou J.** Perinatal lethality with kidney and pancreas defects in mice with a targetted Pkd1 mutation. *Nat Genet* 17: 179–181, 1997.
21. **Martinez-Maldonado M, Yium JJ, Eknoyan G, Suki WN.** Adult polycystic kidney disease: studies of the defect in urine concentration. *Kidney Int* 2: 107–113, 1972.
22. **McDill BW, Li SZ, Kovach PA, Ding L, Chen F.** Congenital progressive hydronephrosis (cph) is caused by an S256L mutation in aquaporin-2 that affects its phosphorylation and apical membrane accumulation. *Proc Natl Acad Sci USA* 103: 6952–6957, 2006.
23. **Mochizuki T, Wu G, Hayashi T, Xenophontos SL, Veldhuisen B, Saris JJ, Reynolds DM, Cai Y, Gabow PA, Pierides A, Kimberling WJ, Breuning MH, Deltas CC, Peters DJ, Somlo S.** PKD2, a gene for polycystic kidney disease that encodes an integral membrane protein. *Science* 272: 1339–1342, 1996.
24. **Murakami M, Nakagawa M, Olson EN, Nakagawa O.** A WW domain protein TAZ is a critical coactivator for TBX5, a transcription factor implicated in Holt-Oram syndrome. *Proc Natl Acad Sci USA* 102: 18034–18039, 2005.
25. **Murakami M, Tominaga J, Makita R, Uchijima Y, Kurihara Y, Nakagawa O, Asano T, Kurihara H.** Transcriptional activity of Pax3 is co-activated by TAZ. *Biochem Biophys Res Commun* 339: 533–539, 2006.
26. **Nagy A, Gertsenstein M, Vintersten K, Behringer R.** *Manipulating the Mouse Embryo: A Laboratory Manual* (3rd ed.). Cold Spring Harbor, NY: Cold Spring Harbor Laboratory, 2003.
27. **Nakagawa O, Nakagawa M, Richardson JA, Olson EN, Srivastava D.** HRT1, HRT2, and HRT3: a new subclass of bHLH transcription factors marking specific cardiac, somitic, and pharyngeal arch segments. *Dev Biol* 216: 72–84, 1999.
28. **Nielsen S, Frøkiær J, Marples D, Kwon TH, Agre P, Knepper MA.** Aquaporins in the kidney: from molecules to medicine. *Physiol Rev* 82: 205–244, 2002.
29. **Onuchic LF, Furu L, Nagasawa Y, Hou X, Eggermann T, Ren Z, Bergmann C, Senderek J, Esquivel E, Zeltner R, Rudnik-Schoneborn S, Mrug M, Sweeney W, Avner ED, Zerres K, Guay-Woodford LM, Somlo S, Germino GG.** PKHD1, the polycystic kidney and hepatic disease 1 gene, encodes a novel large protein containing multiple immunoglobulin-like plexin-transcription-factor domains and parallel beta-helix 1 repeats. *Am J Hum Genet* 70: 1305–1317, 2002.
30. **Park KS, Whitsett JA, Di Palma T, Hong JH, Yaffe MB, Zannini M.** TAZ interacts with TTF-1 and regulates expression of surfactant protein-C. *J Biol Chem* 279: 17384–17390, 2004.
31. **Shao X, Johnson JE, Richardson JA, Hiesberger T, Igarashi P.** A minimal Ksp-cadherin promoter linked to a green fluorescent protein reporter gene exhibits tissue-specific expression in the developing kidney and genitourinary tract. *J Am Soc Nephrol* 13: 1824–1836, 2002.
32. **The European Polycystic Kidney Disease Consortium.** The polycystic kidney disease 1 gene encodes a 14 kb transcript and lies within a duplicated region on chromosome 16. *Cell* 77: 881–894, 1994.
33. **The International Polycystic Kidney Disease Consortium.** Polycystic kidney disease: the complete structure of the PKD1 gene and its protein. *Cell* 81: 289–298, 1995.
34. **Thurlbeck WM.** Measurement of pulmonary emphysema. *Am Rev Respir Dis* 95: 752–764, 1967.
35. **Tian Y, Kolb R, Hong JH, Carroll J, Li D, You J, Bronson R, Yaffe MB, Zhou J, Benjamin T.** TAZ promotes PC2 degradation through a $SCF^{\beta\text{-}Trcp}$ E3 ligase complex. *Mol Cell Biol* 27: 6383–6395, 2007.
36. **Vainio S, Lin Y.** Coordinating early kidney development: lessons from gene targeting. *Nat Rev Genet* 3: 533–543, 2002.
37. **Ward CJ, Hogan MC, Rossetti S, Walker D, Sneddon T, Wang X, Kubly V, Cunningham JM, Bacallao R, Ishibashi M, Milliner DS, Torres VE, Harris PC.** The gene mutated in autosomal recessive polycystic kidney disease encodes a large, receptor-like protein. *Nat Genet* 30: 259–269, 2002.
38. **Wert SE, Yoshida M, LeVine AM, Ikegami M, Jones T, Ross GF, Fisher JH, Korfhagen TR, Whitsett JA.** Increased metalloproteinase activity, oxidant production, and emphysema insurfactant protein D gene-inactivated mice. *Proc Natl Acad Sci USA* 97: 5972–5977, 2000.
39. **Witzgall R.** The proximal tubule phenotype and its disruption in acute renal failure and polycystic kidney disease. *Exp Nephrol* 7: 15–19, 1999.
40. **Yu J, McMahon AP, Valerius MT.** Recent genetic studies of mouse kidney development. *Curr Opin Genet Dev* 14: 550–557, 2004.
41. **Zegers MM, O'Brien LE, Yu W, Datta A, Mostov KE.** Epithelial polarity and tubulogenesis in vitro. *Trends Cell Biol* 13: 169–176, 2003.

INTERNAL MEDICINE

□ CASE REPORT □

Non-Infectious Bronchiolitis as an Early Pulmonary Complication of Hematopoietic Stem Cell Transplantation

Hidenori Kage[1], Tadashi Kohyama[1], Hiroshi Kitagawa[1], Daiya Takai[2], Yoshinobu Kanda[3], Nobuya Ohishi[1] and Takahide Nagase[1]

Abstract

Pulmonary complications occur in up to 60% of patients after hematopoietic stem cell transplantation (HSCT), causing significant morbidity and mortality. Among them, non-infectious bronchiolitis is considered a late complication in the form of bronchiolitis obliterans. We report a patient who developed non-infectious bronchiolitis within four weeks after undergoing HSCT for biphenotypic leukemia. Chest CT revealed centrilobular nodules that were reminiscent of diffuse panbronchiolitis, and lymphocytic bronchiolitis was confirmed by biopsy. Infection and bronchiolitis obliterans were ruled out, and the bronchiolitis resolved when leukemia relapsed. This case suggests that bronchiolitis may be another early, non-infectious pulmonary complication of HSCT.

Key words: bronchiolitis, hematopoietic stem cell transplantation, diffuse panbronchiolitis

(DOI: 10.2169/internalmedicine.47.0456)

Introduction

Hematopoietic stem cell transplantation (HSCT) is used to treat hematological, neoplastic, autoimmune, and genetic diseases, often providing prolonged survival. However, complications are common in the lung; they occur in up to 60% of patients, and account for more than 30% of all transplantation-related deaths (1). They are classified as infectious or non-infectious, and a higher proportion of non-infectious complications have accounted for morbidity and mortality in recent years because the incidence of infection has diminished with effective prophylaxis. Several non-infectious pulmonary complications have been recognized: pulmonary edema, engraftment syndrome, diffuse alveolar hemorrhage, idiopathic pneumonia syndrome, veno-occlusive disease, organizing pneumonia, and bronchiolitis obliterans (BO) (1, 2). BO usually develops after the first 100 days post-transplant, and bronchiolitis other than BO have not been recognized as an early, non-infectious complication of HSCT. Here, we report a case of non-infectious bronchiolitis distinct from BO that developed within the first month of HSCT.

Case Report

A 19-year-old man developed dyspnea, impaired hemostasis, and arthralgia of the lower limbs. Blood tests revealed WBC 198,000/μL, Hb 5.1 g/dL, Plt 15,000/μL. He was admitted for suspected leukemia. Bone marrow aspiration revealed that 67% of nucleated cells were blasts, which were positive for CD10, CD13, CD14, CD19, CD20, CD22, CD33, CD34, HLA-DR, and myeloperoxidase, and a diagnosis of acute biphenotypic leukemia of B cell and myeloid lineage was made according to the European Group of Immunological Classification of Leukemias criteria (3). Two courses of chemotherapy consisting of 170 mg/day of cytarabine on days 1-7 and 20 mg/day of idarubicin on days 5-7 resulted in induction failure, as did two courses of high-dose cytarabine of 6,800 mg/day on days 1-4 and 12 mg/day of mitoxantrone on days 1-2. On-disease allogeneic peripheral blood stem cell transplantation from a completely HLA-

[1]Department of Respiratory Medicine, The University of Tokyo, Tokyo, [2]Department of Clinical Laboratory, The University of Tokyo, Tokyo and [3]Division of Hematology, Omiya Medical Center, Jichi Medical School, Omiya
Received for publication July 17, 2007; Accepted for publication September 21, 2007
Correspondence to Dr. Hidenori Kage, kageh-tky@umin.ac.jp

DOI: 10.2169/internalmedicine.47.0456

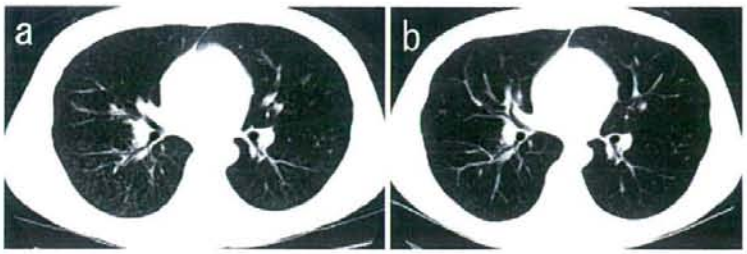

Figure 1. **a) Chest CT on day 25 after transplantation, showing small, diffuse, centrilobular nodules, consistent with bronchiolitis. b) Chest CT on day 46, showing that the nodules have regressed.**

matched sibling [HLA-A (31, 33), B (51, 58), and DR (0301, 0802)] was performed. Pre-transplant paranasal sinus radiograph, chest CT, and spirometry were normal. The conditioning regimen was 2 Gy of total body irradiation twice a day on days -6 to -4 for a total of 12 Gy, and 3,500 mg/day of cyclophosphamide on days -3 and -2. As prophylaxis against graft-versus-host disease (GVHD), he was given 170 mg/day of cyclosporine starting from day -1, and 17 mg of methotrexate on day1 and 12 mg/day on days 3 and 6. Cefepime, vancomycin, micafungin, and acyclovir were given as prophylaxes against infection. CD34-positive peripheral blood stem cells were infused at a dose of 4.4×10^6 cells/kg. Engraftment was confirmed on day 23. On the same day, erythema of the palms and soles were noted, and grade 1 acute GVHD was diagnosed.

A fever of 37.6 degrees, purulent sputum, and dyspnea developed on day 24. On auscultation, lungs were clear. Serum fungal antigens for *Aspergillus*, *Cryptococcus*, and *Candida*, and the cytomegalovirus (CMV) pp65 antigenemia assay were negative. Chest radiograph showed diffuse nodular shadows in both lower lung fields, and sinus X-ray showed fluid in the maxillary sinuses. Bone marrow aspiration on day 30 revealed no blasts, confirming remission. Chest CT on day 32 revealed diffuse, bilateral centrilobular nodules with a predominance in the lower lung fields (Fig. 1A), and sinus CT showed fluid and mucosal thickening of the frontal, maxillary, ethmoidal, and sphenoid sinuses, together reminiscent of diffuse panbronchiolitis (DPB). Arterial blood gas showed pH 7.42, PaO_2 75 Torr, and $PaCO_2$ 40 Torr while breathing ambient air. Pulmonary function tests showed declines in FEV_1, from 4.1 L to 2.4 L, and in FEV_1%, from 91% to 67%, and an increase in $\dot{V}50/\dot{V}25$, from 1.9 to 4.3, indicating significant airflow obstruction. %VC, %RV, %TLC, and RV/TLC all declined from 99% to 90%, from 132% to 80%, from 95% to 78%, and from 29% to 21%, respectively. Diffusing capacity was unchanged. Analysis of broncho-alveolar lavage fluid (BALF) showed total cell counts of 58×10^5 cells/ml with differential cell counts of 25% macrophages, 50% lymphocytes, and 25% eosinophils. Of the lymphocytes, 95% were CD3-positive T cells, and the CD4/8 ratio was 0.70. The peripheral blood white blood cell count was 6,500/μl, and the leukocyte differentials showed 42% neutrophils, 31% eosinophils, 4% basophils, 18% monocytes, and 5% lymphocytes. Bacterial, mycobacterial, and fungal cultures of the BALF were negative, as were the polymerase chain reaction assays for *Aspergillus*, *Pneumocystis jiroveci*, CMV, respiratory syncytial virus, parainfluenza virus, and adenovirus, ruling out infection. Histological examination of trans-bronchial lung biopsy showed lymphocytic bronchitis and bronchiolitis with involvement of adjacent alveoli (Fig. 2). Very few eosinophils were seen. The infiltrating lymphocytes were CD8-positive T cells. The histological findings were not indicative of any infection or bronchiolitis obliterans.

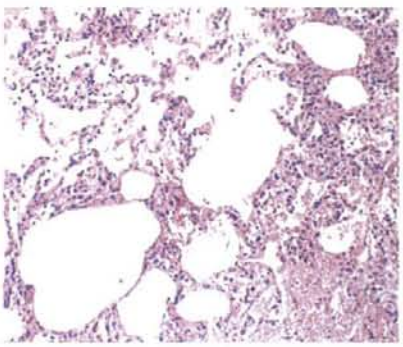

Figure 2. **Transbronchial biopsy (Hematoxylin and Eosin staining, ×100) shows lymphocytic bronchiolitis with involvement of the adjacent alveoli.**

Chest CT on day 46 showed that the lesions had regressed without any treatment (Fig. 1B). On the same day, leukemia cells were found in the peripheral blood, indicating disease relapse, and resolution of GVHD was also observed. The patient died of leukemia on day 64.

Discussion

We have described a case of non-infectious lymphocytic bronchiolitis that developed within a month of HSCT. Chest CT showed centrilobular nodules, pulmonary function tests showed airflow limitation without a decrease in diffusing capacity, and biopsy confirmed the presence of lymphocytic bronchiolitis. There was no evidence of infection, and the clinical picture was quite different from any of the well-

described non-infectious pulmonary complications of HSCT: pulmonary edema, peri-engraftment respiratory distress syndrome, diffuse alveolar hemorrhage, idiopathic pneumonia syndrome, veno-occlusive disease, organizing pneumonia, or BO (1, 2). The present case suggests that bronchiolitis may represent another early, non-infectious pulmonary complication of HSCT.

We do not consider the present case to be BO for three reasons. First, BO usually develops after the first 100 days after transplantation (4). Second, the typical CT findings of BO are air trapping, small airway thickening, or bronchiectasis, not centrilobular nodules (4). Third, biopsy findings did not show any fibrosis or eosinophilic scarring of the bronchioles resulting in narrowing of the lumen, suggestive of BO (5). It has been reported that airflow obstruction develops in the early stages after HSCT without any finding suggestive of BO (6). Therefore, it is possible that some cases of BO are sequelae of early bronchiolitis. Early bronchiolitis may have previously gone mostly unnoticed because of its mild clinical course.

The significance of an increase of eosinophils in the BAL fluid is unclear because only a few eosinophils were seen in biopsy specimens. This discrepancy is sometimes seen in diffuse lung diseases; however, what it indicates is not known. We consider that eosinophils had less of a role compared to lymphocytes based on the histological findings.

The chest CT finding of diffuse, centrilobular nodules with a lower lobe predominance together with clinical syndromes of purulent sputum, dyspnea, sinusitis, and airflow limitation was reminiscent of diffuse panbronchiolitis (DPB), a disease with chronic inflammation of the respiratory bronchioles most often seen in East Asians (7). However, it is clear he did not have DPB because there was no airflow obstruction and chest CT was normal before transplantation. It is possible that bronchiolitis and sinusitis share a common etiology, causing a sinobronchial syndrome, but infection was never ruled out. Therefore, the significance of sinusitis is unclear.

As a complication of HSCT, there have previously been several pathological descriptions of airway disease other than BO. Beschorner et al examined autopsy material from 59 patients with a mean survival of 48 days after receiving bone marrow transplants, and found that 15 had lymphocytic bronchitis (8). Yousem reviewed lung biopsy specimens and described lymphocytic bronchitis or bronchiolitis, distinct from BO, with cellular interstitial pneumonia as one of the manifestations of pulmonary GVHD (9). There have also been case reports of lymphocytic pneumonitis, but not bronchiolitis (10, 11). To our knowledge, this is the first clinical report on early, non-infectious, non-BO bronchiolitis complicating HSCT.

The pathogenesis of the well-recognized, early, non-infectious pulmonary complications have not yet been fully elucidated, but proposed mechanisms include conditioning-related toxicities, immune-mediated injury, and occult infection (1). The pathogenesis of non-infectious bronchiolitis remains obscure. Beschorner et al reported that the development of lymphocytic bronchitis was significantly correlated with the presence of GVHD (8), which is in agreement with the report of Yousem (9) and that using a rat model (12). On the other hand, some have suggested that lymphocytic bronchitis is unrelated to GVHD, using canine models (13). In the present case, because infection was effectively ruled out, and because the bronchiolitis was resolved without any treatment as leukemia relapsed and GVHD subsided, an immune-mediated injury in which the donor lymphocytes attack the recipient airway cells, may be the most plausible explanation.

In conclusion, the present case suggests that bronchiolitis may be considered a distinct form of early non-infectious pulmonary complication of HSCT.

References

1. Kotloff RM, Ahya VN, Crawford SW. Pulmonary complications of solid organ and hematopoietic stem cell transplantation. Am J Respir Crit Care Med **170**: 22-48, 2004.
2. Sirithanakul K, Salloum A, Klein JL, Soubani AO. Pulmonary complications following hematopoietic stem cell transplantation: diagnostic approaches. Am J Hematol **80**: 137-146, 2005.
3. Bene MC, Castoldi G, Knapp W, et al. Proposals for the immunological classification of acute leukemias. European Group for the Immunological Characterization of Leukemias (EGIL). Leukemia **9**: 1783-1786, 1995.
4. Filipovich AH, Weisdorf D, Pavletic S, et al. National Institutes of Health consensus development project on criteria for clinical trials in chronic graft-versus-host disease: I. Diagnosis and staging working group report. Biol Blood Marrow Transplant **11**: 945-956, 2005.
5. Shulman HM, Kleiner D, Lee SJ, et al. Histopathologic diagnosis of chronic graft-versus-host disease: National Institutes of Health Consensus Development Project on Criteria for Clinical Trials in Chronic Graft-versus-Host Disease: II. Pathology Working Group Report. Biol Blood Marrow Transplant **12**: 31-47, 2006.
6. Chien JW, Martin PJ, Flowers ME, Nichols WG, Clark JG. Implications of early airflow decline after myeloablative allogeneic stem cell transplantation. Bone Marrow Transplant **33**: 759-764, 2004.
7. Azuma A, Kudoh S. Diffuse panbronchiolitis in East Asia. Respirology **11**: 249-261, 2006.
8. Beschorner WE, Saral R, G.M. Hutchins GM, Tutschka PJ, Santos GW. Lymphocytic bronchitis associated with graft-versus-host disease in recipients of bone-marrow transplants. N Engl J Med **299**: 1030-1036, 1978.
9. Yousem SA. The histological spectrum of pulmonary graft-versus-host disease in bone marrow transplant recipients. Hum Pathol **26**: 668-675, 1995.
10. Atkinson K, Turner J, Biggs JC, Dodds A, Concannon S. An acute pulmonary syndrome possibly representing acute graft-versus-host disease involving the lung interstitium. Bone Marrow Transplant **8**: 231-234, 1991.
11. Bolanos-Meade J, Ioffe O, Hey JC, Vogelsang GB, Akpek G. Lymphocytic pneumonitis as the manifestation of acute graft-versus-host disease of the lung. Am J Hematol **79**: 132-135, 2005.

DOI: 10.2169/internalmedicine.47.0456

12. Workman DL, Clancy J Jr. Interstitial pneumonitis and lymphocytic bronchiolitis/bronchitis as a direct result of acute lethal graft-versus-host disease duplicate the histopathology of lung allograft rejection. Transplantation **58**: 207-213, 1994.

13. O'Brien KD, Hackman RC, Sale GE, et al. Lymphocytic bronchitis unrelated to acute graft-versus-host disease in canine marrow graft recipients. Transplantation **37**: 233-238, 1984.

ARTICLE IN PRESS
+ MODEL

Respiratory Medicine (2008) xx, 1–8

available at www.sciencedirect.com

ScienceDirect

journal homepage: www.elsevier.com/locate/rmed

Clarithromycin inhibits fibroblast migration

Tadashi Kohyama [a,*], Yasuhiro Yamauchi [a], Hajime Takizawa [b], Susumu Itakura [a], Sumiko Kamitani [a], Jun Kato [a], Takahide Nagase [a]

[a] *Department of Respiratory Medicine, The University of Tokyo, Graduate School of Medicine, 7-3-1 Hongo Bunkyo-ku, Tokyo 113-8655, Japan*
[b] *Fourth Department of Internal Medicine, Teikyo University, School of Medicine, Kawasaki, Japan*

Received 13 March 2008; accepted 30 June 2008

KEYWORDS
Fibroblast;
Macrolide;
Clarithromycin;
Migration

Summary
The aim of the current study was to investigate the effect of 14-membered ring macrolide clarithromycin (CAM) on migration induced by human plasma fibronectin (HFn) or on contraction of human fetal lung fibroblasts (HFL-1).
Methods and results: Using the blindwell chamber technique, CAM (10^{-5} M) inhibited the migration of HFL-1 60.2 ± 4.0% ($p < 0.05$). Other antibiotics, such as ampicillin, minocycline or azithromycin had no effects on HFL-1 migration. The effect of CAM was concentration dependent. HFL-1 migration, stimulated by TXA_2 analog was also inhibited by CAM. Clarithromycin had no effect on HFL-1 mediated gel contraction that was another function of fibroblast at the wound area.
Conclusions: Clarithromycin may contribute to the regulation of the wound healing response following injury by inhibiting fibroblast migration. These results could represent the therapeutic benefits of CAM.

Introduction

After tissue injury, fibroblast migration from surrounding peri-wound connective tissue into the site of wound area and fibroblast contraction at wound area plays an important role in repairing process. Under normal circumstances, fibroblasts are quiescent mesenchymal cells. However, in some inflammatory processes, fibroblasts become activated and excess number of their migration would cause replacement of normal parenchymal elements of tissue to fibrosis.[1] These changes can distort normal tissue architectural relationship, can compromise organ function and can cause fibrosis. One of the therapeutic objectives in fibrotic disease is to reduce the local inflammatory response through the reduction of excess migration and contraction of fibroblast.

The macrolide is a group of antibiotics which have unique large macrocyclic lactone ring. Macrolide inhibits bacterial protein biosynthesis by binding to the subunit 50S of the bacterial ribosome. Macrolide is effective against Gram-positive cocci, mycoplasma, mycobacteria, and chlamydia.

* Corresponding author. Tel.: +81 03 3815 5411; fax: +81 03 3815 5954.
E-mail address: koyama-tky@umin.ac.jp (T. Kohyama).

0954-6111/$ - see front matter © 2008 Elsevier Ltd. All rights reserved.
doi:10.1016/j.rmed.2008.06.020

Please cite this article in press as: Kohyama T et al., Clarithromycin inhibits fibroblast migration, Respiratory Medicine (2008), doi:10.1016/j.rmed.2008.06.020

Among them, 14-membered ring macrolides, however, have curious effects on inflammatory processes. Low dose erythromycin therapy improves the survival or lung function of patient with intractable diseases, such as diffuse panbronchiolitis (DPB) which is mostly recognized in Asian and cystic fibrosis which is most common inherited disease in Caucasian.[2,3] According to the data of inhibition of inflammatory cytokine productions,[4–6] changing the Th1/Th2 cytokine ratio[3] and effectiveness in cancer studies,[7–9] macrolide effects might be immunomodulatory activities. In vivo study also shows that macrolide might prevent the lung injury and fibrosis in bleomycin-challenged mouse.[10]

However, the precise mechanism of 14-membered ring macrolide has not been elucidated clearly yet. The current study evaluated the potential effects of CAM on fibroblast-mediated repair responses by using *in vitro* models of tissue remodeling. Our findings, therefore, support the notion that CAM may play a role in the remedy of remodeling of the lung.

Materials and methods

Materials

Clarithromycin was generously provided by Taisho Pharmaceutical Co. (Tokyo, Japan). Ampicillin (ABPC), minocycline (MINO) and azithromycin (AZM) were purchased from SIGMA (St. Louis, MO). KT5720 was purchased from Calbiochem (San Diego, CA). Ampicillin (10^{-2} M), MINO (2×10^{-2} M) was dissolved into dH_2O, CAM (5×10^{-3} M) and AZM(10^{-3} M) were dissolved into 100% ethanol and KT5720 was dissolved into dimethylsulfoxide (DMSO) at 10^{-2} M for stock reagents.

According to the reports of previous experiments,[11,5,4,12] we chose the concentration of each drugs as follows: MINO (10^{-6} M); ABPC (10^{-5} M); CAM (10^{-5} M); AZM (10^{-5} M). Those concentrations were around the clinical plasma levels achieved pharmacologically after using standard dosage.

Tissue culture supplements and media were purchased from GIBCO (Life Technologies, Grand Island, NY). Fetal calf serum (FCS) was purchased from Biofluid (Rockville, MD). Human fetal lung fibroblasts (HFL-1) were obtained from the American Type Culture Collection (Rockville, MD). A second strain of human fetal lung fibroblasts (WI-38) was purchased from Health Science Research Resources Bank (Osaka, Japan). The cells were cultured in 100 mm tissue culture dishes (FALCON; Becton–Dickinson Labware, Lincoln Park, NJ) in Dulbecco's modified Eagle medium (DMEM, Gibco, Grand Island, NY), supplemented with 10% FCS, 50 U/ml penicillin G sodium and 50 μg/ml streptomycin sulfate (penicillin–streptomycin, GIBCO) in a humidified atmosphere at 37 °C and 5% CO_2. The fibroblasts were routinely passaged every 4 or 5 days and cells were used between passage 13 and 21 in all experiments. Subconfluent fibroblasts were removed from the dishes by treatment with 0.05% trypsin in 0.53 mM ethylenediaminetetraacetic acid and stop the reaction by soybean trypsin inhibitor (GIBCO). After centrifuging to remove the trypsin inhibitor, cells were re-suspended in DMEM without serum.

Cell toxicity examination

Preliminary, MTT assay was performed to test the toxicity of reagents and diluents. Briefly, after being cultured for 6 h with each reagent in 96 well culture plate, the medium were discarded and 100 μl MTT solution (200 μg/ml in DMEM) per well was added. After another 4 h incubation, MTT solution were discarded and 100 μl of DMEM per well was added to melt formazan crystal. The OD values were read at 630 nm wavelength.

Fibroblast migration

HFL-1 and WI-38 migrations were assessed by the Boyden blindwell chamber system[13] using 48-well chambers (Nucleopore, Cabin John, MD). The chemoattractant fibronectin was placed in the bottom chamber. The upper and lower portions of the chamber were separated by the 8 μm pore filter (Nucleopore, Pleasanton, CA) coated with 0.1% gelatin (Bio Rad, Hercules, CA). The top manifold was placed and human fetal lung fibroblasts (1.0×10^6 ml in DMEM without serum) were loaded into the upper wells of the chamber with the desired concentration of CAM or

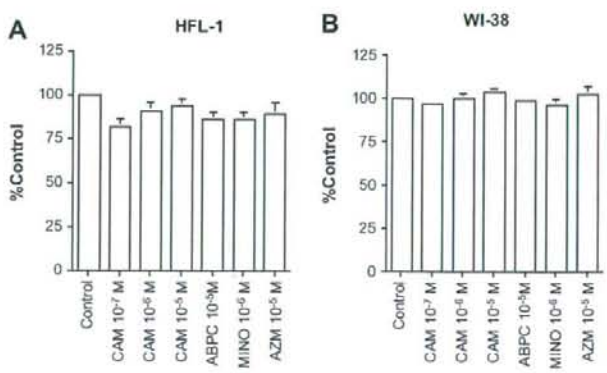

Figure 1 MTT assay. Vertical axis, expressed as percentage of control. Horizontal axis: conditions. (A) HFL-1, (B) WI-38. Data shown are means + SEM for three separate experiments. Each conditions for MTT assay in triplicate.

Please cite this article in press as: Kohyama T et al., Clarithromycin inhibits fibroblast migration, Respiratory Medicine (2008), doi:10.1016/j.rmed.2008.06.020

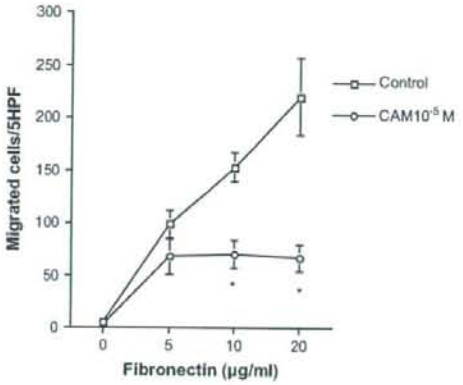

Figure 2 Inhibition of fibroblast migration by CAM. Migration of HFL-1 fibroblasts was measured with blindwell assay system using human fibronectin with or without the CAM (10^{-5} M). Vertical axis, fibroblast migration expressed as number of cells migrated per 5 high-power fields; horizontal axis: concentration of fibronectin. Data shown are means ± SEM for representative data from three separate experiments. Each experiments for migration in triplicate. ($^*p < 0.05$).

other additives. The chamber was then incubated at 37 °C in a moist, 5% CO_2 atmosphere. Except the time course experiment chambers were incubated for 6 h, after which the cells on the top of the filter were removed by scraping. The filter was then fixed, stained with Diff Quik stain (International reagents CORP, Kobe, Japan), and mounted on a glass microscope slide. Migration was assessed by counting the number of cells in 5 high-power fields using a light microscope. Triplicate wells were prepared in each experiment for every condition. Replica experiments were performed with separate cultures of cells on separate occasions.

Collagen gel contraction assay

To test the CAM effect on contractility of fibroblast, another function of fibroblast, fibroblast-mediated gel contraction was measured according to a method developed by Bell and coworkers.[14] Collagen gels were prepared as described previously.[15] Briefly, Type I collagen that was extracted from rat tail,[16] distilled water, 4 × DMEM and fibroblast suspensions were mixed by pipetting so that the final mixture resulted in 0.75 mg/ml of collagen, 3×10^5 fibroblasts/ml gel and a physiologic ionic strength of 1 × DMEM. A 500 μl portion of the gel solution was then cast into each well of a 24-well tissue culture plate (FALCON). After gelation, the gels were released into 60 mm tissue culture dishes (FALCON) containing 5 ml of DMEM with designed concentration of CAM. The floating gels were cultured for up to 5 days, and the ability of the fibroblasts to contract the gels was determined by quantifying the area of the gels daily using an image analyzer (ATTO, Tokyo, Japan).

Statistical analysis

Samples with multiple comparisons were analyzed for significance using analysis of variance (ANOVA). Pair-wise comparisons were analyzed by independent two sample *t*-test where the critical value is adjusted for multiple comparisons by the Tukey test. ($p < 0.05$) Summary data are expressed as mean ± SEM.

Results

MTT assay showed that each concentration of the reagents and diluents using these experiments were not toxic for the fibroblasts (Fig. 1).

The migration was measured by using the blindwell assay system. Fibronectin put in the lower wells directed the

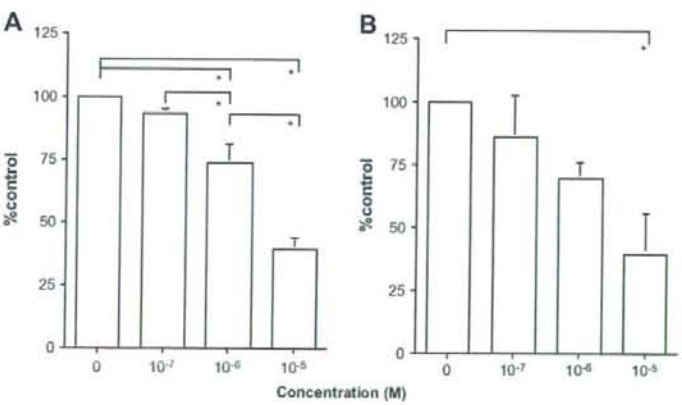

Figure 3 Inhibition of fibroblast migration by CAM: concentration dependence. Fibronectin (20 μg/ml) was used as the chemoattractant. Clarithromycin was added to the fibroblasts at various concentrations immediately before the cells were placed in the top wells of the chemotaxis chamber. (A) HFL-1, (B) WI-38. Vertical axes: fibroblast migration expressed as a percentage of that control. Horizontal axis: CAM concentration. Data shown are means + SEM for triplicate separate experiments, each assayed for chemotactic activity in triplicate. ($^*p < 0.05$).

Please cite this article in press as: Kohyama T et al., Clarithromycin inhibits fibroblast migration, Respiratory Medicine (2008), doi:10.1016/j.rmed.2008.06.020

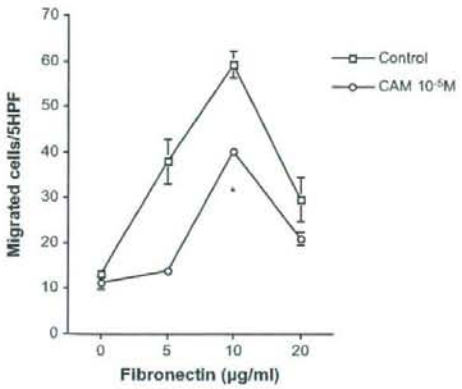

Figure 4 Clarithromycin effect on the chemokinesis of HFL-1. Same concentrations of human fibronectin were placed both above and below the filter. There is no chemoattractant gradient. Vertical axes: fibroblast migration expressed as number of cells migrated per 5 high-power fields; Horizontal axis: fibronectin concentration of both sides. Data shown are means ± SEM for representative data from three separate experiments. Each experiments for migration in triplicate. ($^*p < 0.05$).

HFL-1 migration in concentration dependent fashion. Clarithromycin (10^{-5} M) added in the top wells inhibited the HFL-1 migration at 10 and 20 μg/ml of fibronectin (Fig. 2).

Clarithromycin inhibited the fibronectin (20 μg/ml) directed migration in concentration dependent manner. The inhibitory effect reached significant by 10^{-6} M of CAM

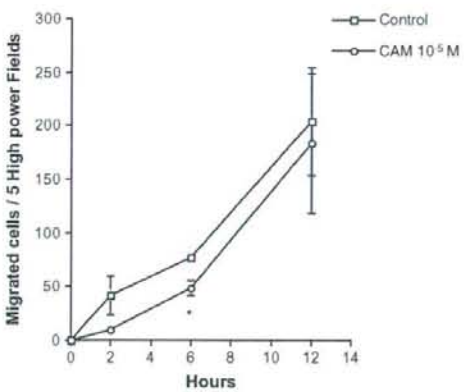

Figure 5 Inhibition of fibroblast migration by CAM: time course. Fibronectin (20 μg/ml) was used as the chemoattractant. Clarithromycin was added to the fibroblasts in the top wells at various concentrations. The chambers were incubated and after varying times, removed for staining and counting. Vertical axis: fibroblast migration expressed as number of cells migrated per 5 high-power fields; horizontal axis: time in hours. Data shown are means ± SEM for representative data from three separate experiments. Each experiment for migration in triplicate ($^*p < 0.05$).

on HFL-1 (control, 100%; CAM 10^{-6} M, 73.7 ± 7.3%, $p < 0.05$) and by 10^{-5} M of CAM on WI-38 (control, 100%; CAM 10^{-5} M, 46.2 ± 15.5%, $p < 0.05$) (Fig. 3).

To determine if CAM inhibit chemokinesis, same concentrations of human fibronectin were placed both above and below the filter. The meaning of this experiment shows there is no chemoattractant gradient (chemokinesis) even in the presence of increasing concentrations of fibronectin above and below the filter. Clarithromycin also inhibited chemokinesis (at fibronectin 10 μg/ml; control, 59.3 ± 2.9; CAM 10^{-5} M, 40.3 ± 0.9%, $p < 0.05$) (Fig. 4).

In the time course assay, the accumulation of the HFL-1 continued to increase even at the end point we tested (12 h). Clarithromycin (10^{-5} M) inhibited the HFL-1 migration at 6 h (control, 76.0 ± 5.6; CAM, 10^{-5} M 48.0 ± 7.1%, $p < 0.05$) (Fig. 5).

To elucidate the inhibitory effects of CAM on the activated fibroblast as in the inflammatory area, we tested the CAM effect on the fibroblast activated by TXA_2 analog U46619. Clarithromycin (10^{-5} M) significantly inhibited the U46619 (2×10^{-7} nM) activated fibroblasts migration (control = 100%; U46619, 130.3 ± 8.2; U46619 plus CAM 10^{-5} M, 53.1 ± 2.5%, $p < 0.05$) (Fig. 6).

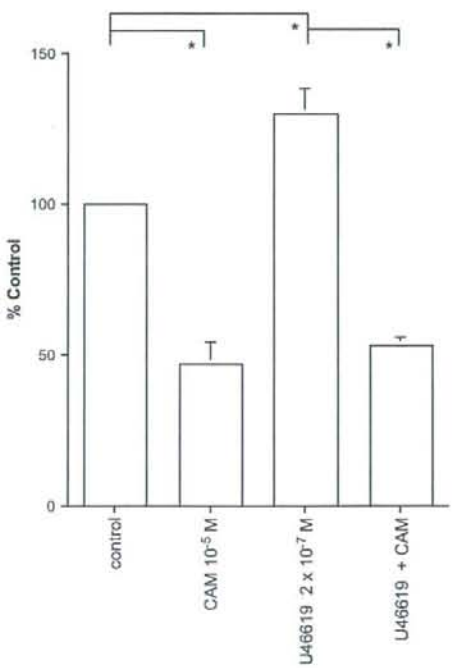

Figure 6 Effect of CAM on stimulatory cells by TXA_2 analog U46619. HFL-1 were pre-incubated with U46619 (2×10^{-7} M) in monolayer culture for 1 h and then harvested for migration. Fibronectin (20 g/ml) was used as chemoattractant. Clarithromycin (10^{-5} M) was added to the fibroblasts in the top wells with 2×10^{-7} M of U46619. Vertical axis, fibroblast migration expressed as percentage of control. Data are means + SEM for triplicate cultures each assayed for migration in triplicate. ($^*p < 0.05$).

Please cite this article in press as: Kohyama T et al., Clarithromycin inhibits fibroblast migration, Respiratory Medicine (2008), doi:10.1016/j.rmed.2008.06.020

We have tried to check another antibiotics Ampicillin (ABPC) (10^{-5} M), minocycline (MINO) (10^{-6} M) and azithromycin (AZM) (10^{-5} M) effects on human lung fibroblast migration. Among them CAM but other antibiotics inhibited the migration of HFL-1. (control = 100%; ABPC 90.7 ± 5.1%; MINO, 105.6 ± 9.7%; CAM 45.8 ± 4.6% $p < 0.05$; AZM 99.5 ± 15.3%) (Fig. 7A). As azithromycin is one of the macrolides, we confirmed its effect with several concentrations. Azithromycin had no effect on HFL-1 migration (Fig. 7B).

Among the fibroblast functions in the wound area, contractility is also important for repair and remodeling process. To elucidate the CAM effect on it, we have used gel contraction assay system. Clarithromycin had no effect on fibroblast contraction in the gel (Fig. 8).

There is no clear mechanism report of CAM effect on fibroblast migrations. Most of the reagents which inhibit the fibroblast migrations are related to the activation of protein kinase A.[17,18] To determine if the inhibition of migration toward fibronectin by CAM is by way of PKA pathway, we assessed the PKA inhibitor KT5720 with CAM. As there is the report which showed that KT5720 block the inhibitory effect of PGD_2 on fibroblast migration,[18] we put the PGD_2 examination as control. KT5720 did not block the inhibitory effect of CAM on HFL-1 migration (Fig. 9).

Discussion

The current study demonstrates that CAM was capable of inhibiting fibroblast migration to human fibronectin. The effects by CAM were concentration dependent. Clarithromycin also inhibited the TXA_2 analog U46619 stimulated migration of HFL-1. Moreover, CAM inhibited both human lung fibroblast chemotaxis and chemokinesis. Clarithromycin had no effect on contractility of fibroblast that is important function for end stage of wound healing.

The accumulation of fibroblasts to the wound site is often a key event in both normal repair and in the development of fibrosis.

In the process of it, fibroblast migration, proliferation and contraction are essential events. Under normal repair process, adequate numbers of fibroblasts migrate to the wound area.

However, an excess accumulation of fibroblasts and excess deposition of extracellular matrix produced by fibroblast results in replacement of the normal tissue parenchyma with fibrotic scar, which results in irreversible distortion of the lung's architecture and compromising organ function.[19,1]

Idiopathic pulmonary fibrosis (IPF) is a chronic, progressive and fetal lung disorder. The mean prognosis after diagnosis is ranging from 3 to 5 years.[20] The treatments employed currently are steroids and cytotoxic agents, however, both of them have not been proven to prolong survival or improve pulmonary function among patients with IPF. The critical phenomenon which related prognosis is ongoing epithelial damage and persistent fibroblastic proliferation.[21]

In this context, the reagent which controls the fibroblast function might be a good medicine.

Clarithromycin, a 14-membered ring macrolide, is known as an antibiotic. Recently we have used this medicine as immunomodulatory drug. This opinion is supported by in vitro and in vivo data. Clarithromycin decreases the production of cytokines,[4–6] changes the Th1/Th2 cytokine ratio[3] and prevents the lung injury and fibrosis in bleomycin-challenged mouse.[10]

These reports will give us hints to explore that clarithromycin might make biological actions on the cells which are important for wound healing or remodeling in the inflammatory milieu.

Our data showed that CAM inhibited fibroblast migration. This is important effect for inhibiting the remodeling.

Fibronectin of plasma is chemotactic for HFL-1 and WI-38.

For the reason mentioned below, we used the fibronectin for chemoattractant of fibroblasts. Fibronectin, one of the extracellular matrixes, is mainly produced by fibroblasts[22] and soluble in plasma and tissues. Fibronectin

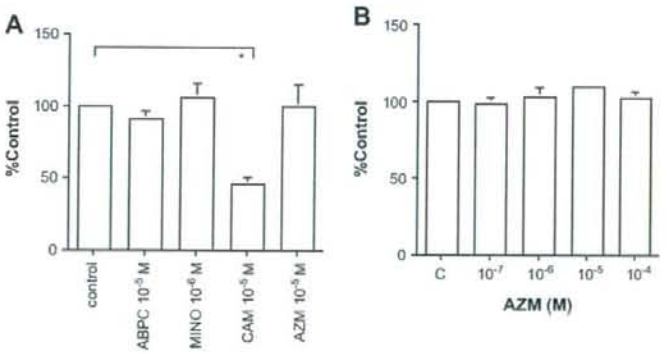

Figure 7 Effects of other antibiotics on fibroblast chemotaxis. HFL-1 migration was performed in the Boyden blind well chamber assay system. (A) Ampicillin (ABPC) (10^{-5} M), minocycline (MINO) (10^{-6} M), CAM (10^{-9} M) and azithromycin (AZM) (10^{-5} M) were added to the top of each well. (B) Several concentration of AZM was tested. Vertical axis, fibroblast migration expressed as percentage of control. Horizontal axis: each condition. Data are means + SEM for triplicate cultures each assayed for migration in triplicate. (*$p < 0.05$).

Please cite this article in press as: Kohyama T et al., Clarithromycin inhibits fibroblast migration, Respiratory Medicine (2008), doi:10.1016/j.rmed.2008.06.020

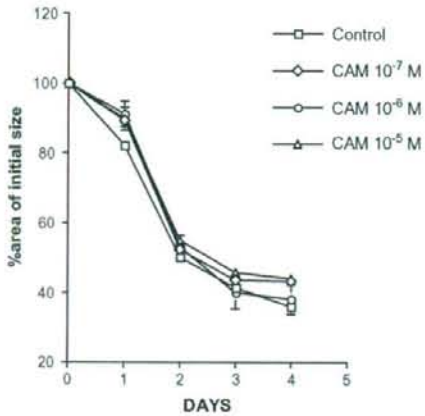

Figure 8 Effect of CAM on collagen gel contraction. HFL-1 was cast into gel and floated on the conditioned media. The size of gel area was measured every day. Vertical axis: gel size as percentage of initial area; horizontal axis, time after release (day). Data shown are means ± SEM for representative data from three separate experiments. Each experiments for contraction in triplicate. ($^*p < 0.05$).

content of the wound matrix is much higher than that of the adjacent tissue.[23] It is reasonable for fibroblast and inflammatory cells, such as neutrophil and monocyte, to migrate into the wound area.[24–28] Recruiting the inflammatory cells is important for management of infection and removal of tissue debris in the wound area. Fibronectin helps platelet to attach to collagen[29] and enmeshed in blood clots[28] at the defect of tissue. Moreover fibronectin mediate fibroblasts attachment to collagen.[30] Taken together, these findings suggest that fibronectin is very important for wound healing.

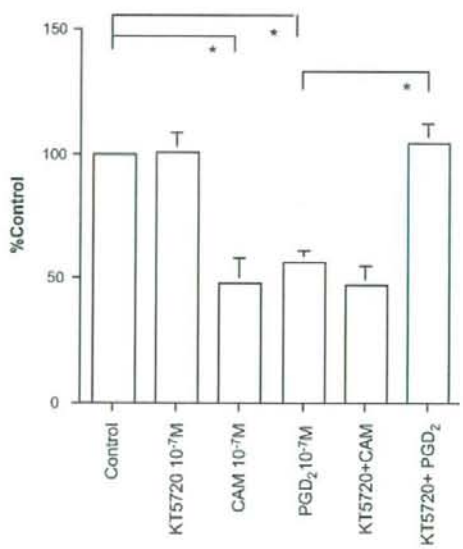

Figure 9 Effect of protein kinase A inhibitor on CAM reducing HFL-1 migration. HFL-1 migration was performed in the Boyden blind well chamber assay system. Protein kinase A inhibitor KT5720 was added to the upper wells with or without CAM. KT5720 effect on PGD_2 was the positive control of this assay. ($^*p < 0.05$).

Our data clearly showed that CAM inhibited the migration of even the stimulated fibroblast by TXA_2 analog U46619.

TXA_2 is an inflammatory mediator that can modulate a variety of important biologic functions, including coagulation and vasomotor and bronchomotor reactivity.[31] Several report shows that adequate physiologic concentration of U46619 (TXA_2 analog) is 10^{-8}–10^{-6} M.[32,33] Our previous study showed that 2×10^{-7} nM of U46619 showed highest activity of fibroblast migration,[34] then we chose this concentration for stimulator of migration.

Clarithromycin had no effect on fibroblast contraction which is another function and final process of wound healing. Not like other drugs which effect on fibroblast migration,[35,36] CAM effect might be limited in early part of wound healing process.

The mechanism of CAM effect on the fibroblast migration is not clear. Previous studies demonstrate that several mediators that inhibit the lung fibroblast migration are related to the protein kinase A (PKA).[17,37] The current study indicated that CAM effect but PGD_2 on HFL-1 migration was related to protein kinase A (Fig. 9). We had also tried but fail to show the effect of CAM on the p38 activity that is related to cell migration[38] (data not shown). Continuous study of CAM mechanism would be required.

There are no clinical trials with CAM for treatment of fibroblast related to wound healing such as IPF. However, there are in vivo experiment reports which show macrolide effects on mouse models of idiopathic pulmonary fibrosis. Fourteen-membered ring macrolides inhibit bleomycin-induced acute lung injury.[39,40] Recent studies have shown that both COPD and asthma are also associated with fibrosis of small airways.[41,42] We might be able to expand the treatment territory with CAM even to COPD and asthma, and to use CAM. There is a possibility of using CAM for treatment of these diseases.

In summary, the current study demonstrated that clarithromycin could inhibit fibroblast migration. This effect of CAM could potentially reduce the tissue remodeling and relieve the diseases of fibrotic.

Conflict of interest and sources of funding

The authors declare that they had no conflict of interest.

Acknowledgements

The authors thank Miss Makiko Kase for her excellent technical assistance.

References

1. Rennard SI, Jaurand MC, Bignon J, Kawanami O, Ferrans VJ, Davidson J, et al. Role of pleural mesothelial cells in the

Please cite this article in press as: Kohyama T et al., Clarithromycin inhibits fibroblast migration, Respiratory Medicine (2008), doi:10.1016/j.rmed.2008.06.020

production of the submesothelial connective tissue matrix of lung. *Am Rev Respir Dis* 1984;**130**:267–74.
2. Kudoh S, Azuma A, Yamamoto M, Izumi T, Ando M. Improvement of survival in patients with diffuse panbronchiolitis treated with low-dose erythromycin. *Am J Respir Crit Care Med* 1998;**157**:1829–32.
3. Pukhalsky AL, Shmarina GV, Kapranov NI, Kokarovtseva SN, Pukhalskaya D, Kashirskaja NJ. Anti-inflammatory and immunomodulating effects of clarithromycin in patients with cystic fibrosis lung disease. *Mediators Inflamm* 2004;**13**:111–7.
4. Takizawa H, Desaki M, Ohtoshi T, Kikutani T, Okazaki H, Sato M, et al. Erythromycin suppresses interleukin 6 expression by human bronchial epithelial cells: a potential mechanism of its anti-inflammatory action. *Biochem Biophys Res Commun* 1995;**210**:781–6.
5. Takizawa H, Desaki M, Ohtoshi T, Kawasaki S, Kohyama T, Sato M, et al. Erythromycin modulates IL-8 expression in normal and inflamed human bronchial epithelial cells. *Am J Respir Crit Care Med* 1997;**156**:266–71.
6. Kohyama T, Takizawa H, Kawasaki S, Akiyama N, Sato M, Ito K. Fourteen-member macrolides inhibit interleukin-8 release by human eosinophils from atopic donors. *Antimicrob Agents Chemother* 1999;**43**:907–11.
7. Sasaki M, Ito T, Kashima M, Fukui S, Izumiyama N, Watanabe A, et al. Erythromycin and clarithromycin modulation of growth factor-induced expression of heparanase mRNA on human lung cancer cells in vitro. *Mediators Inflamm* 2001;**10**:259–67.
8. Mikasa K, Sawaki M, Kita E, Hamada K, Teramoto S, Sakamoto M, et al. Significant survival benefit to patients with advanced non-small-cell lung cancer from treatment with clarithromycin. *Chemotherapy* 1997;**43**:288–96.
9. Sakamoto M, Mikasa K, Majima T, Hamada K, Konishi M, Maeda K, et al. Anti-cachectic effect of clarithromycin for patients with unresectable non-small cell lung cancer. *Chemotherapy* 2001;**47**:444–51.
10. Li Y, Azuma A, Takahashi S, Usuki J, Matsuda K, Aoyama A, et al. Fourteen-membered ring macrolides inhibit vascular cell adhesion molecule 1 messenger RNA induction and leukocyte migration: role in preventing lung injury and fibrosis in bleomycin-challenged mice. *Chest* 2002;**122**:2137–45.
11. Watanabe A, Anzai Y, Niitsuma K, Saito M, Yanase K, Nakamura M. Penetration of minocycline hydrochloride into lung tissue and sputum. *Chemotherapy* 2001;**47**:1–9.
12. Morris DL, De Souza A, Jones JA, Morgan WE. High and prolonged pulmonary tissue concentrations of azithromycin following a single oral dose. *Eur J Clin Microbiol Infect Dis* 1991;**10**:859–61.
13. Boyden S. The chemotactic effect of mixtures of antibody and antigen on polymorphonuclear leucocytes. *J Exp Med* 1962; **115**:453–66.
14. Bell E, Ivarsson B, Merrill C. Production of a tissue-like structure by contraction of collagen lattices by human fibroblasts of different proliferative potential in vitro. *Proc Natl Acad Sci U S A* 1979;**76**:1274–8.
15. Mio T, Adachi Y, Romberger DJ, Ertl RF, Rennard SI. Regulation of fibroblast proliferation in three dimensional collagen gel matrix. *In Vitro Cell Dev Biol* 1996;**32**:427–33.
16. Elsdale T, Bard J. Collagen substrata for studies on cell behavior. *J Cell Biol* 1972;**54**:626–37.
17. Kohyama T, Ertl RF, Valenti V, Spurzem J, Kawamoto M, Nakamura Y, et al. Prostaglandin E(2) inhibits fibroblast chemotaxis. *Am J Physiol Lung Cell Mol Physiol* 2001;**281**: L1257–63.
18. Kohyama T, Liu XD, Wen FQ, Kim HJ, Takizawa H, Rennard SI. Prostaglandin D2 inhibits fibroblast migration. *Eur Respir J* 2002;**19**:684–9.
19. Hunninghake WC, Garret KC, Richerson HB, Fantone JC, Ward PA, Rennard SI, et al. Pathogenesis of the granulomatous lung disease (state of art). *Am Rev Respir Dis* 1984;**130**: 476–96.
20. Panos RJ, Mortenson RL, Niccoli SA, King Jr TE. Clinical deterioration in patients with idiopathic pulmonary fibrosis: causes and assessment. *Am J Med* 1990;**88**:396–404.
21. King Jr TE, Schwarz MI, Brown K, Tooze JA, Colby TV, Waldron Jr JA, et al. Idiopathic pulmonary fibrosis: relationship between histopathologic features and mortality. *Am J Respir Crit Care Med* 2001;**164**:1025–32.
22. Adachi Y, Mio T, Takigawa K, Striz I, Romberger DJ, Spurzem JR, et al. Fibronectin production by cultured human lung fibroblasts in three-dimensional collagen gel culture. *In Vitro Cell Dev Biol Anim* 1998;**34**:203–10.
23. Grinnell F, Billingham RE, Burgess L. Distribution of fibronectin during wound healing in vivo. *J Invest Dermatol* 1981;**76**: 181–9.
24. Gauss-Muller V, Kleinman HK, Martin GR, Schiffmann E. Role of attachment factors and attractants in fibroblast chemotaxis. *J Lab Clin Med* 1980;**96**:1071–80.
25. Postlethwaite AE, Keski-Oja J, Balian G, Kang AH. Induction of fibroblast chemotaxis by fibronectin. Localization of the chemotactic region to a 140,000-molecular weight non-gelatin-binding fragment. *J Exp Med* 1981;**153**:494–9.
26. Doillon CJ, Silver FH. Collagen-based wound dressing: effects of hyaluronic acid and fibronectin on wound healing. *Biomaterials* 1986;**7**:3–8.
27. Jarstrand C, Ahlgren T, Berghem L. Fibronectin increases the motility, phagocytosis and NBT (nitroblue tetrazolium)-reduction of granulocytes. *J Clin Lab Immunol* 1982;**8**:59–63.
28. Grinnell F. Fibronectin and wound healing. *J Cell Biochem* 1984;**26**:107–16.
29. Hynes RO, Ali IU, Destree AT, Mautner V, Perkins ME, Senger DR, et al. A large glycoprotein lost from the surfaces of transformed cells. *Ann N Y Acad Sci* 1978;**312**:317–42.
30. Rennard SI, Chen YF, Robbins RA, Gadek JE, Crystal RG. Fibronectin mediates cell attachment to C1q: a mechanism for the localization of fibrosis in inflammatory disease. *Clin Exp Immunol* 1983;**54**:239–47.
31. Ogletree ML. Overview of physiological and pathophysiological effects of thromboxane A2. *Fed Proc* 1987;**46**:133–8.
32. Mene P, Abboud HE, Dunn MJ. Regulation of human mesangial cell growth in culture by thromboxane A2 and prostacyclin. *Kidney Int* 1990;**38**:232–9.
33. Studer RK, Craven PA, DeRubertis FR. Thromboxane stimulation of mesangial cell fibronectin synthesis is signalled by protein kinase C and modulated by cGMP. *Kidney Int* 1994; 46:1074–82.
34. Kohyama T, Liu X, Wen FQ, Kim HJ, Takizawa H, Rennard SI. Potentiation of human lung fibroblast chemotaxis by the thromboxane A(2) analog U-46619. *J Lab Clin Med* 2002;**139**: 43–9.
35. Kohyama T, Wyatt TA, Liu X, Wen FQ, Kobayashi T, Fang Q, et al. PGD2 modulates fibroblast-mediated native collagen gel contraction. *Am J Respir Cell Mol Biol* 2002; **27**:375–81.
36. Kohyama T, Liu X, Wen FQ, Zhu YK, Wang H, Kim HJ, et al. PDE4 inhibitors attenuate fibroblast chemotaxis and contraction of native collagen gels. *Am J Respir Cell Mol Biol* 2002;**26**:694–701.
37. Kohyama T, Liu X, Kim HJ, Kobayashi T, Ertl RF, Wen FQ, et al. Prostacyclin analogs inhibit fibroblast migration. *Am J Physiol Lung Cell Mol Physiol* 2002;**283**:L428–32.
38. Heuertz RM, Tricomi SM, Ezekiel UR, Webster RO. C-reactive protein inhibits chemotactic peptide-induced p38 mitogen-activated protein kinase activity and human neutrophil movement. *J Biol Chem* 1999;**274**:17968–74.
39. Azuma M, Nishioka Y, Aono Y, Inayama M, Makino H, Kishi J, et al. Role of alpha1-acid glycoprotein in therapeutic antifibrotic

Please cite this article in press as: Kohyama T et al., Clarithromycin inhibits fibroblast migration, Respiratory Medicine (2008), doi:10.1016/j.rmed.2008.06.020

effects of imatinib with macrolides in mice. *Am J Respir Crit Care Med* 2007;**176**:1243–50.
40. Kawashima M, yatsunami J, Fukuno Y, Nagata M, Tominaga M, Hayashi S. Inhibitory effects of 14-membered ring macrolide antibiotics on bleomycin-induced acute lung injury. *Lung* 2002;**180**:73–89.
41. Hoshino M, Nakamura Y, Sim J, Shimojo J, Isogai S. Bronchial subepithelial fibrosis and expression of matrix metalloproteinase-9 in asthmatic airway inflammation. *J Allergy Clin Immunol* 1998;**102**:783–8.
42. Saetta M, Turato G. Airway pathology in asthma. *Eur Respir J Suppl* 2001;34:18s–23s.

Please cite this article in press as: Kohyama T et al., Clarithromycin inhibits fibroblast migration, Respiratory Medicine (2008), doi:10.1016/j.rmed.2008.06.020

Platelet-Activating Factor Production in the Spinal Cord of Experimental Allergic Encephalomyelitis Mice via the Group IVA Cytosolic Phospholipase A_2-Lyso-PAFAT Axis[1]

Yasuyuki Kihara,* Keisuke Yanagida,* Kayo Masago,* Yoshihiro Kita,* Daisuke Hishikawa,* Hideo Shindou,* Satoshi Ishii,*† and Takao Shimizu[2]*

Platelet-activating factor (PAF; 1-*O*-alkyl-2-acetyl-*sn*-glycero-3-phosphocholine) plays a critical role in inflammatory disorders including experimental allergic encephalomyelitis (EAE), an animal model for multiple sclerosis (MS). Although PAF accumulation in the spinal cord (SC) of EAE mice and cerebrospinal fluid of MS patients has been reported, little is known about the metabolic processing of PAF in these diseases. In this study, we demonstrate that the activities of phospholipase A_2 (PLA_2) and acetyl-CoA:lyso-PAF acetyltransferase (LysoPAFAT) are elevated in the SC of EAE mice on a C57BL/6 genetic background compared with those of naive mice and correlate with disease severity. Correspondingly, levels of groups IVA, IVB, and IVF cytosolic PLA_2s, group V secretory PLA_2, and LysoPAFAT transcripts are up-regulated in the SC of EAE mice. PAF acetylhydrolase activity is unchanged during the disease course. In addition, we show that LysoPAFAT mRNA and protein are predominantly expressed in microglia. Considering the substrate specificity and involvement of PAF production, group IVA cytosolic PLA_2 is likely to be responsible for the increased PLA_2 activity. These data suggest that PAF accumulation in the SC of EAE mice is profoundly dependent on the group IVA cytosolic PLA_2/LysoPAFAT axis present in the infiltrating macrophages and activated microglia. *The Journal of Immunology*, **2008, 181: 5008–5014.**

Platelet-activating factor (PAF[3]; 1-*O*-alkyl-2-acetyl-*sn*-glycero-3-phosphocholine), a potent proinflammatory lipid mediator (1), is believed to be synthesized via two distinct pathways, the de novo and remodeling pathways (Ref. 2 and see Fig. 1). The latter pathway is primarily involved in the synthesis of PAF by stimulated inflammatory cells such as murine peritoneal cells (3, 4) and human granulocytes (5). The initiation of the remodeling pathway requires membrane phospholipid hydrolysis by phospholipase A_2s (PLA_2; EC 3.1.1.4) that supply lyso-PAF, a precursor of PAF. Acetyl-CoA:lyso-PAF acetyltransferase (LysoPAFAT; EC 2.3.1.67) converts lyso-PAF into PAF. PAF activates the PAF receptor (PAFR), a member of the superfamily of G protein-coupled receptors (6), and elicits a variety of biological responses (1). PAF is rapidly degraded by PAF acetylhydrolases (PAF-AH; EC 3.1.1.47) that cleave the acetyl group at the *sn*-2 position to reform lyso-PAF (7).

PLA_2 are classified into three groups: group VI calcium-independent PLA_2s (iPLA_2s), secretory PLA_2s (sPLA_2s), and group IV cytosolic PLA_2s (cPLA_2) (8). Group IVA cPLA_2 preferentially liberates arachidonic acid from 2-arachidonoyl-phospholipids (8, 9). The released arachidonic acids are in turn converted into PGs and leukotrienes via the arachidonic acid cascade (10). It is thought that group VI iPLA_2 and some types of sPLA_2s have the potential to initiate the arachidonic acid cascade, even though these enzymes lack significant substrate specificity (8). Group IVA cPLA_2 is also essential for producing PAF, since PAF synthesis is significantly diminished in calcium ionophore-stimulated macrophages derived from group IVA cPLA_2-deficient mice as compared with those from wild-type mice (11). Recently, our group has successfully overcome the long-standing challenges of cloning and identifying LysoPAFAT (12), a critical enzyme that produces PAF. We termed the enzyme LsoPAFAT/LPCAT2 (lysophosphatidylcholine acyltransferase 2) (12). We have demonstrated that murine macrophages and neutrophils express LysoPAFAT/LPCAT2 mRNA and possess a LysoPAFAT activity (3, 12). Furthermore, LysoPAFAT/LPCAT2 mRNA is induced by the ligands for TLRs 4 and 9 in murine macrophages (12). These results imply that LysoPAFAT plays a crucial role in the enhanced PAF production in inflammatory disorders.

Multiple sclerosis (MS) is considered to be a $CD4^+$ T cell-mediated autoimmune disease and is characterized by inflammation and demyelination in the CNS (13). The mechanism of MS,

*Department of Biochemistry and Molecular Biology, Faculty of Medicine, University of Tokyo, Tokyo, Japan; and †Precursory Research for Embryonic Science and Technology of Japan Science and Technology Agency, Tokyo, Japan

Received for publication October 9, 2007. Accepted for publication July 21, 2008.

The costs of publication of this article were defrayed in part by the payment of page charges. This article must therefore be hereby marked *advertisement* in accordance with 18 U.S.C. Section 1734 solely to indicate this fact.

[1] This work was supported, in part, by Grants-in-Aid from the Ministry of Education, Science, Culture, Sports and Technology of Japan (to T. S. and S. I.), a grant to the Respiratory Failure Research Group from the Ministry of Health, Labour and Welfare, Japan (to S. I.), Grants-in-Aid for Comprehensive Research on Aging and Health from the Ministry of Health, Labour and Welfare, Japan (to S. I.), the Kato Memorial Trust for Nambyo Research (to S. I.), and the Japanese Society for the Promotion of Science (research fellowships to Y.Ki., D.H., and K.Y.). H.S., S.I., and T.S. were supported by the Center for NanoBio Integration (University of Tokyo).

[2] Address correspondence and reprint requests to Dr. Takao Shimizu, Department of Biochemistry and Molecular Biology, Faculty of Medicine, University of Tokyo, 7-3-1 Hongo, Bunkyo, Tokyo 113-0033, Japan. E-mail address: tshimizu@m.u-tokyo.ac.jp

[3] Abbreviations used in this paper: PAF, platelet-activating factor; PLA_2, phospholipase A_2; LysoPAFAT, acetyl-CoA:lyso-PAF acetyltransferase; LysoPAFAT/LPCAT2, LysoPAFAT/lysophosphatidylcholine acyltransferase 2; lyso-PAF, 1-*O*-alkyl-*sn*-glycero-3-phosphocholine; PAFR, PAF receptor; PAF-AH, PAF acetylhydrolase; PC, phosphatidylcholine; iPLA_2, calcium-independent PLA_2; sPLA_2, secretory PLA_2; cPLA_2, cytosolic PLA_2; MS, multiple sclerosis; EAE, experimental allergic encephalomyelitis; MOG, myelin oligodendrocyte glycoprotein; SC, spinal cord; ESI-MS/MS, electrospray ionization-tandem mass spectrometry; LPCAT1, lysophosphatidylcholine acyltransferase 1; APMSF, amidinophenylmethanesulfonyl fluoride; GFAP, glial fibrillary acidic protein.

however, remains obscure because of limited access to the CNS at various phases of MS. An animal model, experimental allergic encephalomyelitis (EAE), is indispensable for a better understanding of MS pathology (14). Howat et al. (15) suggested an involvement of PAF in EAE for the first time. We have found that PAFR-KO mice immunized with myelin oligodendrocyte glycoprotein (MOG) peptide 35–55 (MOG_{35-55}) show less severe symptoms than wild-type mice (16). Group IVA $cPLA_2$ deficiency protects mice from EAE pathology (17). We also have reported that there is a correlation between the PAF level in the spinal cord (SC) and EAE symptoms (16), which is consistent with PAF levels in the cerebrospinal fluid of relapsing-remitting MS patients (18). In the SC of EAE mice, PAF seems to exist in the nanomolar range, which is adequate to provoke biological responses through the PAFR (6). Moreover, the level of PAFR transcript is up-regulated in MS lesions (19) and the CNS of EAE-induced SJL and C57BL/6 mice (16, 20). The elevated levels of both PAF and PAFR transcripts probably worsen the MS/EAE pathology. EAE, as an animal model of MS, is useful for understanding the roles of PAF in MS (14), since studies on PAF in MS lesions are in accordance with those in EAE lesions (16, 18–20). However, the metabolic processing of PAF and involvement of LysoPAFAT/LPCAT2 in EAE pathology are largely unknown. In the present study, we have induced EAE in C57BL/6 mice with the MOG_{35-55} peptide and revealed that PAF accumulation in SCs of EAE mice is dependent on the up-regulation of the expression and activities of both group IVA $cPLA_2$ and LysoPAFAT. This is the first report suggesting the involvement of LysoPAFAT/LPCAT2 in the disease models.

Materials and Methods

Induction of EAE

EAE was induced in 8-wk-old C57BL/6 female mice. The maintenance of the facility and the use of animals were in full compliance with the University of Tokyo Ethics Committee for Animal Experiments. MOG_{35-55} (MEVGWYRSPFSRVVHLYRNGK), corresponding to the fragment of mouse MOG from aa 35–55, was synthesized by Sigma-Aldrich. Mice were immunized s.c. in the flank with 300 μg of MOG_{35-55} peptide in 0.1 ml of PBS and 0.1 ml of CFA containing 0.4 mg of *Mycobacterium tuberculosis* (H37Ra; Difco Laboratories) on days 0 and 7 and injected i.p. with 250 ng of pertussis toxin (List Biological Laboratories) on days 0 and 2. Mice were scored as follows: 0, no sign; 0.5, mild loss of tail tone; 1.0, complete loss of tail tone; 1.5, mildly impaired righting reflex; 2.0, abnormal gait and/or impaired righting reflex; 2.5, hind limb paresis; 3.0, hind limb paralysis; 3.5, hind limb paralysis with hind body paresis; 4.0, hind and fore limb paralysis; 4.5, moribund; and 5.0, death. To understand the EAE pathology, we divided the disease course into induction, acute, and chronic phases in accordance with the clinical symptoms as previously described (Ref. 16 and Fig. 2A).

Quantification of PAF

PAF and eicosanoid levels were estimated simultaneously as previously described (21, 22). The results of the eicosanoid levels will be published elsewhere (Y. Kihara, S. Ishii, Y. Kita, S. Uematsu, S. Akira, and T. Shimizu, unpublished data). SCs of naive mice and EAE mice were removed on days 12, 19, and 32, frozen immediately with liquid nitrogen, and stored at −80°C until use. The frozen tissues (~100 mg) were powdered with an SK-100 mill (Tokken), and lipids were extracted for 60 min at 4°C with methanol containing deuterium-labeled 16:0 PAF (Cayman Chemical) as an internal standard. The extracts were loaded onto Oasis HLB cartridges (30 mg; Waters) preloaded with methanol and 0.03% (v/v) formic acid/H_2O. The cartridges were washed with 0.03% formic acid/H_2O, 15% (v/v) ethanol, and petroleum ether. Lipids were extracted with 100% methanol and PAF levels were quantified by reversed-phase HPLC electrospray ionization (ESI)-tandem mass spectrometry (MS/MS) as described previously (21, 22).

Quantitative real-time PCR

On days 11–12, 18–19, and 30–31, naive and EAE mice were anesthetized with urethane (1.5 g/kg of body; Sigma-Aldrich) and intracardially perfused with 10 ml of ice-cold PBS. The SCs were removed and total RNA was isolated using an RNeasy Mini Kit (Qiagen). The purity and integrity of total RNA were determined by the absorbance at $A_{260/280}$ and gel electrophoresis, respectively. One microgram of total RNA was reverse-transcribed using SuperScript II (Invitrogen Life Technologies) according to the manufacturer's instructions. The RT^2 Profiler PCR Array System for PLA_2 (groups IVA, IVB, IVC, IVD, IVE, and IVF $cPLA_2$s, groups V and X $sPLA_2$s, and group VI $iPLA_2$) was purchased from SuperArray, and quantitative RT-PCR for these PLA_2 mRNAs was performed with a 7500 Fast Real-Time PCR System (Applied Biosystems). The relative abundance of PLA_2 mRNA levels in EAE mice compared with naive mice was calculated by the comparative cycle threshold method using hypoxanthine phosphoribosyltransferase as a normalization control. Quantification of LysoPAFAT, lysophosphatidylcholine acyltransferase 1 (LPCAT1), and β-actin mRNA levels was performed with LightCycler FastStart DNA Master SYBR Green I (Roche) as previously described (12, 23). Results were quantified by using standard curves derived from SCs in the acute phase of EAE.

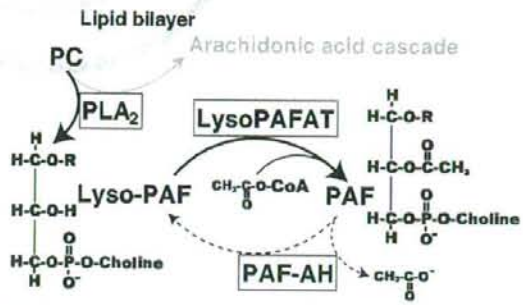

FIGURE 1. PAF production in the remodeling pathway (bold arrow) and degradation pathway (dotted arrow).

Sample preparation for enzyme assays and Western blotting

The SCs of naive mice and EAE mice on days 12, 19, and 34 were removed following perfusion, frozen immediately with liquid nitrogen, and stored at −80°C until use. The tissues (~100 mg) were homogenized with a Physcotoron homogenizer (Microtec) in 500 μl of buffer A (100 mM Tris-HCl (pH 7.4) containing 10.26% sucrose, 20 μM amidinophenylmethanesulfonyl fluoride (APMSF), 5 mM 2-ME, and 1 × Complete Protease Inhibitor Mixture (Roche)). The homogenate was centrifuged at 9,000 × g for 10 min at 4°C and the resulting supernatant was centrifuged at 100,000 × g for 60 min at 4°C. The pellet was resuspended in buffer B (20 mM Tris-HCl (pH 7.4) containing 20 μM APMSF, 5 mM 2-ME, and EDTA-free 1 × Complete Protease Inhibitor Mixture) and stored at −80°C until use. Protein concentrations were determined by the Bradford method using a protein assay solution (Bio-Rad) and BSA (fraction V, fatty acid-free; Sigma-Aldrich) as a standard.

PLA_2 assay

PLA_2 activity was measured by Dole's method with some modifications (24). Briefly, 5 μg of protein (100,000 × g supernatant) was incubated at 37°C for 30 min in a total volume of 0.25 ml of assay buffer (100 mM HEPES-NaOH (pH 7.4) 1 mg/ml BSA, 4 mM $CaCl_2$, and 1 mM DTT) containing mixed micelles (4 μM Triton X-100 and 2 μM 1-palmitoyl-2-[^{14}C]arachidonoyl-phosphatidylcholine (PC) (1.961 GBq/mmol, GE Healthcare BioSciences). The reaction was terminated by adding 1.25 ml of Dole's reagent (isopropanol:n-heptane:sulfuric acid, 78:20:2), followed by the sequential addition of 0.75 ml of n-heptane and 0.5 ml of water. After centrifugation, an aliquot (0.8 ml) of the upper layer was mixed with 120–150 mg of silica gel, which had been preincubated with 0.75 ml of n-heptane. The radioactivity of an aliquot (0.8 ml) was estimated using an LS6500 liquid scintillation counter (Beckman Coulter) in the presence of 1 ml of Microscinti-0 (PerkinElmer).

LysoPAFAT assay

LysoPAFAT activity was measured according to the method of Kume et al. (4, 12, 25), with some modifications. Briefly, 5 μg of protein (100,000 ×

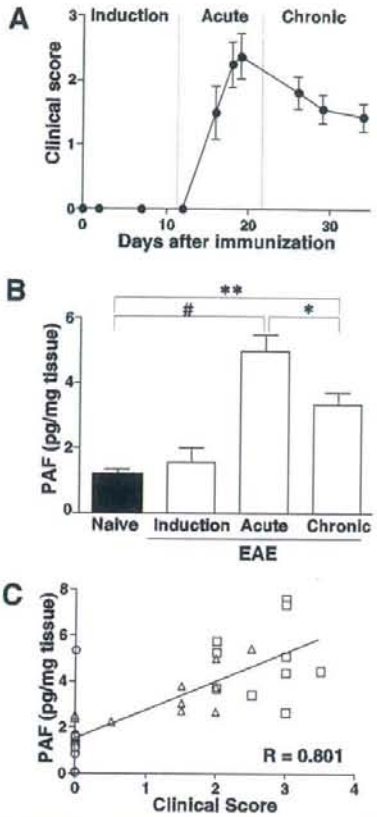

FIGURE 2. Clinical course and PAF levels during EAE. *A*, C57BL/6 female mice were immunized with the MOG_{35-55} peptide. Data are the mean clinical scores ± SEM of eight animals. *B*, PAF levels were determined in SCs of naive mice and EAE mice in the induction, acute, and chronic phases (n = 10 animals). Data represent means ± SEM. #, $p < 0.001$; **, $p < 0.01$; and *, $p < 0.05$ by ANOVA with the Tukey-Kramer test. *C*, PAF levels of naive (●) and EAE mice in the induction (○), acute (□), and chronic (△) phases are positively correlated with the clinical scores ($p < 0.0001$ by the Spearman rank correlation test). Each data point represents the result from a single animal.

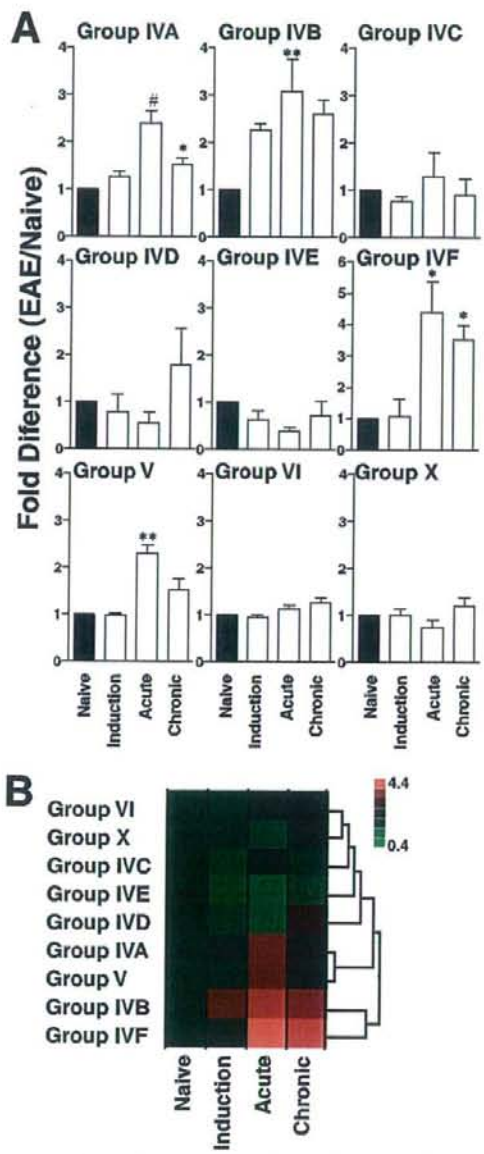

FIGURE 3. PLA_2 mRNA expression in SCs of naive and EAE mice. *A*, Expression of PLA_2 transcripts was quantified by real-time PCR in SCs of naive mice and EAE mice in the induction, acute, and chronic phases (n = 6, 5, 6, and 5 animals, respectively). The relative abundance of PLA_2 mRNA levels in EAE mice compared with naive mice is shown. Data represent means ± SEM. #, $p < 0.001$; **, $p < 0.01$; and *, $p < 0.05$ compared with naive mice by the Kruskal-Wallis test with Dunn's post hoc test. *B*, The relationships among PLA_2 mRNA levels were evaluated by cluster analysis using JMP6 software (Hulinks). The relative expression levels shown in *A* are divided into seven parts and colored from red to green.

g pellet) was incubated at 37°C for 10 min in a total volume of 0.1 ml of reaction mixture (buffer B containing 2 mM $CaCl_2$, 1 mg/ml PC (Sigma-Aldrich), and 100 μM [^{3}H]acetyl-CoA (1.11 GBq/mmol; GE Healthcare BioSciences)) with or without 20 μM lyso-PAF (Cayman Chemical). Subsequently, 122 μl of ice-cold methanol was added to terminate the reaction. The product was bound to 6 mg of C8 resin (Millipore), washed eight times with 55% (v/v) methanol in 20 mM Tris-HCl (pH 7.4), and eluted with 100% methanol. After drying at 50°C for 2 h, the radioactivity was determined using a TopCount microplate scintillation counter (PerkinElmer) in the presence of 200 μl of Microscinti-0. LysoPAFAT activity was calculated by subtracting the radioactivity obtained without lyso-PAF from that obtained with lyso-PAF.

PAF-AH assay

PAF-AH activity was evaluated under the same conditions as reported previously, with minor modifications (26, 27). Briefly, 10 μg of protein (100,000 × g supernatant) was incubated at 37 °C for 30 min in a total volume of 0.25 ml of assay buffer (50 mM Tris-HCl (pH 7.4), 5 mM EDTA, 5 mM 2-ME, and 100 μM [*acetyl*-^{3}H]PAF (85 MBq/mmol; PerkinElmer)). The reaction was stopped by adding 2.5 ml of chloroform/methanol (4:1, v/v), followed by 0.25 ml of water. The radioactivity of an aliquot (0.6 ml) of each water phase was measured with 2 ml of the liquid scintillation mixture, Atomlight (PerkinElmer), to determine the amount of acetyl groups liberated from PAF.

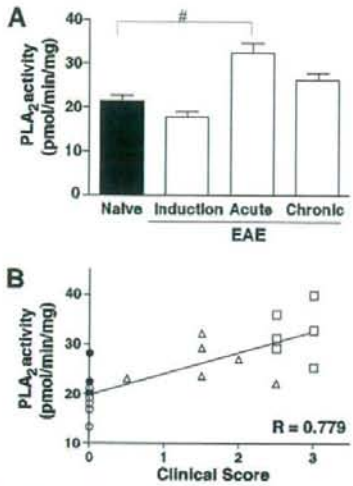

FIGURE 4. PLA_2 activity in SCs of naive and EAE mice. *A*, PLA_2 activity in SCs of naive mice and EAE mice in the induction, acute, and chronic phases ($n = 6$ animals) was measured using mixed micelles containing 1-palmitoyl-2-[^{14}C]arachidonoyl-PC and Triton X-100 in the presence of Ca^{2+} and DTT. Data represent means ± SEM. #, $p < 0.001$ by ANOVA with the Tukey-Kramer test. *B*, PLA_2 activity in naive (●) and EAE mice in the induction (○), acute (□), and chronic (△) phases is positively correlated with the clinical score ($p < 0.0001$ by the Spearman rank correlation test). Each data point represents the result from a single animal.

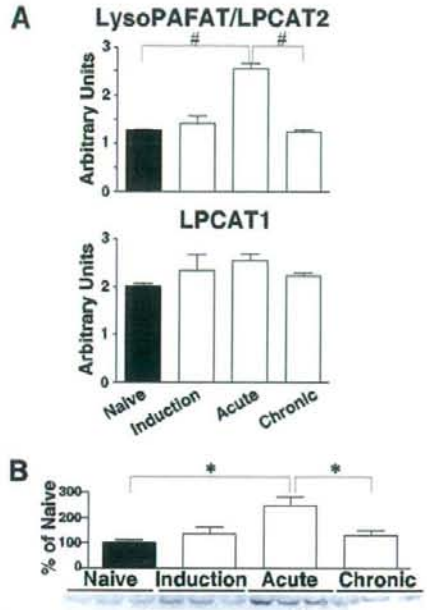

FIGURE 5. LysoPAFAT/LPCAT2 expression in SCs of naive and EAE mice. Expression levels of LysoPAFAT/LPCAT2 and LPCAT1 mRNAs (*A*) and LysoPAFAT/LPCAT2 proteins (*B*) were quantified by real-time PCR and Western blotting with densitometry, respectively, in SCs of naive mice and EAE mice in the induction, acute, and chronic phases ($n = 6$ animals). A representative blot from two independent experiments is shown for LysoPAFAT ($n = 3$ animals). Data represent means ± SEM. #, $p < 0.001$ and *, $p < 0.05$ by ANOVA with the Tukey-Kramer test.

Western blotting

Ten micrograms of protein was resolved by 10% SDS-PAGE and transferred to a Hybond ECL nitrocellulose membrane (GE Healthcare Bio-Sciences). The membrane was blocked with 5% skim milk and incubated with anti-LysoPAFAT antiserum (Immuno-Biological Laboratories). After washing, the membranes were incubated with HRP-linked anti-rabbit IgG (GE Healthcare BioSciences), washed, and then exposed to the Western blotting detection reagents (GE Healthcare BioSciences). The membranes were scanned with a LAS-4000 luminescent image analyzer (Fuji film).

Primary culture

Primary young cortical neurons were prepared from C57BL/6 mouse brains on embryonic day 13 as previously described (28, 29). Primary astrocytes and microglia were obtained from cerebral hemispheres of C57BL/6 mouse brains on postnatal day 1, as previously described, with minor modifications (28–30). Briefly, after a 14-day culture period, astrocytes were purified by two passages. Microglia was prepared as a floating cell suspension and transferred to culture dishes. Unattached cells were removed before isolating total RNA. The purities of astrocytes and microglia were estimated to be >90% and >99%, respectively, by immunostaining for glial fibrillary acidic protein (GFAP) and Iba1. Total RNA (1 μg) was reverse-transcribed as described above.

$CD4^+$ and $CD8^+$ T cells were obtained from spleens of C57BL/6 mice using a MACS magnetic cell separation system (Miltenyi Biotec). The purities of $CD4^+$ and $CD8^+$ T cells were estimated to be >90% by flow cytometry (Beckman Coulter). T cells were stimulated with or without anti-CD3ε Ab (BD Biosciences) for 24 h, followed by reverse transcription of total RNA (100 ng) as described above.

Statistical analysis

Results are expressed as means ± SEM. Data were analyzed statistically by means of ANOVA with the Tukey-Kramer post hoc test, the Kruskal-Wallis test with Dunn's post hoc test, or the Spearman rank correlation test as appropriate, using GraphPad PRISM software. Values of $p < 0.05$ were considered to be statistically significant. Cluster analysis was performed using JMP6 software (Hulinks).

Results

Elevation of PAF levels in SCs of EAE mice

C57BL/6 female mice were immunized with MOG_{35-55} and clinical symptoms were monitored (Fig. 2*A*). All mice developed EAE and the mean maximal clinical score was 2.6 ± 0.16 ($n = 8$ animals). To confirm our previous report, PAF levels in SCs were measured by HPLC-ESI-MS/MS. The SCs were collected from naive mice and immunized mice in the induction, acute, and chronic phases of EAE (Fig. 2*A*). PAF levels were significantly elevated in the acute phase (Fig. 2*B*) and positively correlated with the clinical score ($p < 0.0001$; Fig. 2*C*). Thus, the fluctuation in PAF levels during the disease course was reproduced (16). These results demonstrate that the metabolism of PAF (Fig. 1) in the SC was perturbed by the pathogenesis of EAE. Therefore, we determined the enzymes that synthesize and degrade PAF using EAE mice.

Up-regulation of PLA_2 mRNA expression and activity in SCs of EAE mice

The various PLA_2 (groups IVA, IVB, IVC, IVD, IVE, and IVF $cPLA_2$s, groups V and X $sPLA_2$s, and group VI $iPLA_2$) mRNA levels were determined by quantitative RT-PCR to elucidate the effects of PLA_2s on PAF production. Group IVA $cPLA_2$ and group V $sPLA_2$ mRNA levels were elevated in the acute phase of EAE and decreased in the chronic phase to a level that was still higher than that in naive mice (Fig. 3*A*). The relationships among the mRNA levels were evaluated by cluster analysis that distinguished group IVA $cPLA_2$ and group V $sPLA_2$ from other PLA_2s (Fig. 3*B*). In addition, the poorly characterized groups IVB and IVF

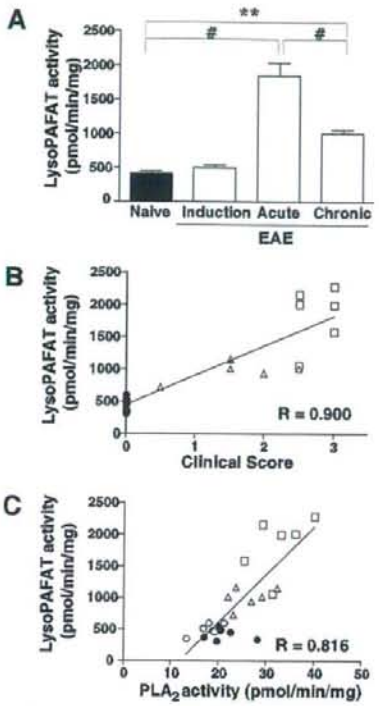

FIGURE 6. LysoPAFAT activity in SCs of naive and EAE mice. *A*, LysoPAFAT activity in SCs of naive mice and EAE mice in the induction, acute, and chronic phases ($n = 6$ animals) was measured as described in *Materials and Methods*. Data represent means ± SEM. #, $p < 0.001$ and **, $p < 0.01$ by ANOVA with the Tukey-Kramer test. *B* and *C*, LysoPAFAT activity in SCs of naive (●) and EAE mice in the induction (○), acute (□), and chronic (△) phases is positively correlated with the clinical score (*B*; $p < 0.0001$ by the Spearman rank correlation test) and PLA_2 activity (*C*; $p < 0.0001$). Each data point represents the results from a single animal.

$cPLA_2$s were up-regulated and clustered together (Fig. 3, *A* and *B*). PLA_2 activity was measured using 1-palmitoyl-2-[^{14}C]arachidonoyl-PC as a substrate with Ca^{2+} and DTT. The enzyme activity increased with the progression of EAE pathology ($p < 0.001$; Fig. 4*A*) and correlated significantly with the clinical score ($p < 0.0001$; Fig. 4B). These results suggest that PAF accumulation in SCs of EAE mice may be due to an up-regulation of PLA_2 and lysoPAFAT (see below).

Enhancement of LysoPAFAT/LPCAT2 expression and activity in SCs of EAE mice

To examine the involvement of LysoPAFAT/LPCAT2, expression levels of the transcripts and proteins were examined in SCs of naive and EAE mice by quantitative RT-PCR and Western blotting, respectively. LysoPAFAT/LPCAT2 transcripts and proteins were elevated in the acute phase and then declined in the chronic phase of EAE (Fig. 5). In contrast, mRNA expression level of the homologous enzyme LPCAT1 was unaltered during the disease course (Fig. 5). In agreement with these observations, the enzyme activities in the acute and chronic phases were higher than those of naive mice ($p < 0.001$; Fig. 6*A*). We found a significantly positive correlation between the clinical score and the LysoPAFAT activity ($p < 0.0001$; Fig. 6*B*). Furthermore, LysoPAFAT activity was positively correlated with PLA_2 activity ($p < 0.001$; Fig. 6*C*). These results suggest that PAF accumulation in SCs of EAE mice is caused by the enhancement of LysoPAFAT/LPCAT2 expression and the corresponding increase in LysoPAFAT activity.

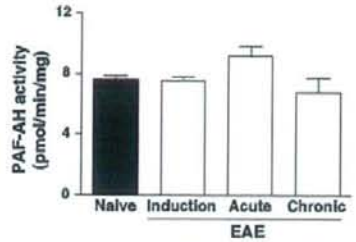

FIGURE 7. PAF-AH activity in SCs of naive and EAE mice. PAF-AH activity in SCs of naive mice and EAE mice in the induction, acute, and chronic phases ($n = 6$ animals) was measured as described in *Materials and Methods*. Data represent means ± SEM.

Unaltered basal PAF-AH activity in SCs of EAE mice

We investigated whether PAF-AH affected the accumulation of PAF in SCs of EAE mice. Although PAF-AH activity appeared to be slightly increased in the acute phase of EAE, the enzyme activity did not change significantly during the disease course (Fig. 7). PAF-AH activity did not correlate with the clinical score, PLA_2 activity, or LysoPAFAT activity (data not shown). Thus, PAF accumulation in SCs of EAE mice may be independent of the PAF degradation system.

LysoPAFAT/LPCAT2 expression in primary cultured murine microglia and astrocytes

We previously demonstrated LysoPAFAT/LPCAT2 mRNA expression in murine brain, macrophages, and neutrophils (12). Its expression was determined by RT-PCR and Western blotting in primary cultured murine neurons, astrocytes, microglia (Fig. 8), $CD4^+$ T cells, and $CD8^+$ T cells (data not shown). We found that LysoPAFAT/LPCAT2 mRNA was expressed in microglia and astrocytes, but not in neurons (Fig. 8*A*). The levels of LysoPAFAT/LPCAT2 transcripts were very low in both T cell subsets, with or without anti-CD3ε Ab stimulation for 24 h (data not shown). LysoPAFAT/LPCAT2 protein expression was observed in microglia, but not in astrocytes (Fig. 8*B*). These results suggest that PAF may

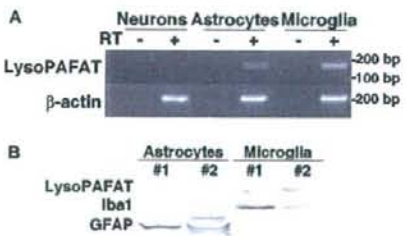

FIGURE 8. LysoPAFAT/LPCAT2 expression in the primary cultured cells of the murine CNS. *A*, LysoPAFAT/LPCAT2 and β-actin mRNA expression in primary cultured neurons, astrocytes, and microglia was determined by RT-PCR. The expected PCR products for LysoPAFAT and β-actin were 167 and 197 bp, respectively. *B*, Expression of LysoPAFAT/LPCAT2, Iba1, and GFAP in primary cultured astrocytes and microglia was determined by Western blotting. Each lane represents cells purified from an individual experiment.

be produced by activated microglia and infiltrating macrophages in SCs of EAE mice.

Discussion

In the present study, we have assessed the metabolic processing of PAF in SCs of naive and EAE mice to explain the enhanced PAF production in EAE mice. In general, accumulation of PAF can be accounted for by the up-regulation of the production system in the remodeling pathway and/or the down-regulation of the degradation system. We have demonstrated that the PAF production system is increased and the degradation system is unchanged in SCs during EAE.

The PAF production system in the remodeling pathway consists of two steps. The first step is production of the PAF precursor lyso-PAF by PLA_2s that hydrolyze the *sn*-2 acyl chain of PC (9) (Fig. 1). Several lines of evidence have suggested that group IVA $cPLA_2$, groups IIA and V $sPLA_2$s, and group VI $iPLA_2$ mRNAs are expressed in the SC of the naive rat (31, 32). In agreement with these studies, we have found that SCs of C57BL/6 mice express these PLA_2 mRNAs, with the exception of group IIA $sPLA_2$ (Fig. 3), which is absent in this mouse strain (33). Because the groups IVA, IVB, and IVF $cPLA_2$s and group V $sPLA_2$ mRNA levels are elevated in the acute phase of EAE (Fig. 3), lipid mediators produced by these four PLA_2s presumably participate in the pathogenesis of EAE. Although little is known about the functions of groups IVB and IVF $cPLA_2$s, it is generally accepted that group IVA $cPLA_2$ and group V $sPLA_2$ stimulate the arachidonic acid cascade (33). Indeed, hierarchical cluster analysis demonstrates the functional analogy of these PLA_2s in EAE pathology (Fig. 3*B*). EAE is not completely ameliorated in PAFR-KO mice (16), whereas group IVA $cPLA_2$ deficiency or treatments with PLA_2 inhibitors protect mice from the EAE pathology (17, 34). Eicosanoid levels were quantified simultaneously and we found that PGE_2 levels were dramatically changed during the disease course (Y. Kihara, S. Ishii, Y. Kita, S. Uematsu, S. Akira, and T. Shimizu, unpublished data). These data suggest that, not only PAF, but also eicosanoids downstream of PLA_2 are critical for the EAE pathology. We have demonstrated the elevation of PLA_2 activity in the acute phase of EAE using 1-palmitoyl-2-[^{14}C]arachidonoyl-PC as a substrate in the presence of Ca^{2+} and DTT (Fig. 4). Since this assay condition is optimized for group IV $cPLA_2$s (35), the elevated PLA_2 activity in the acute phase of EAE may be derived from groups IVA, IVB, and/or IVF $cPLA_2$s. However, groups IVB and IVF $cPLA_2$s have lower PLA_2 activity than group IVA $cPLA_2$ under the present assay conditions (24, 36, 37). Thus, group IVA $cPLA_2$ may be deeply involved in the up-regulation of PLA_2 activity in SCs of EAE mice. Additionally, group IVA $cPLA_2$ is essential for producing PAF, since PAF synthesis is significantly diminished in calcium ionophore-stimulated group IVA $cPLA_2$-deficient macrophages (11). These results suggest that the PAF precursor lyso-PAF is supplied primarily by group IVA $cPLA_2$ during EAE. Because Cunningham et al. (38) reported that $sPLA_2$ activity was up-regulated in urine of EAE rats and MS patients, it may play roles in the EAE pathology. In addition, Bernatchez et al. (39) reported that group V $sPLA_2$ is involved in the PAF production in endothelial cells. Further studies are needed to clarify the roles of group V $sPLA_2$ in EAE lesions.

The second step of the PAF production system is acetylation of lyso-PAF to form PAF by the action of LysoPAFAT, which is critical for the stimulus-dependent formation of PAF (2–4, 12). We have previously shown that LysoPAFAT/LPCAT2 mRNA is expressed in brain, macrophages, and neutrophils (12). Likewise, we have demonstrated the constitutive expression and activity of LysoPAFAT in the SC of naive mice (Figs. 5 and 6). Since LysoPAFAT/LPCAT2 expression is mainly detected in primary cultured microglia by RT-PCR and Western blotting (Fig. 8), microglia may contribute to the production of PAF in the CNS of naive mice for maintaining brain homeostasis (Fig. 9, *left*). A number of inflammatory cells, such as T cells and macrophages, infiltrate the CNS through the broken blood-brain barrier in EAE mice. Furthermore, microglia and astrocytes are activated by cytokines produced by the infiltrating cells (40, 41). The expression and activity of LysoPAFAT were significantly elevated in SCs of EAE mice as compared with those of naive mice (Figs. 5 and 6). Because LysoPAFAT/LPCAT2 is an inducible protein, its expression might be strongly up-regulated in infiltrating macrophages and activated microglia (Fig. 9, *right*). We also have shown that LysoPAFAT activity is correlated with PLA_2 activity (Fig. 6*C*). Kalyvas and David (34) have reported that group IVA $cPLA_2$ is expressed in $CD11b^+$ cells from mice with severe symptoms of EAE. Hence, group IVA $cPLA_2$ and LysoPAFAT appear to be coexpressed in the same cells, such as macrophages/microglia, and to function coordinately in PAF synthesis. In contrast, LysoPAFAT/LPCAT2 mRNA was undetected in T cells stimulation with or without anti-CD3*e* Ab for 24 h (data not shown). These results are in accord with previous reports demonstrating that LysoPAFAT activity is present in macrophages (4, 12), but not in T cells (42). The results are also consistent with our previous report that PAF plays a dominant role in the chronic phase of EAE through the activation of macrophages/microglia (16). Taken together, LysoPAFAT induced in macrophages/microglia plays a crucial role in PAF production in EAE pathology (Fig. 9, *right*).

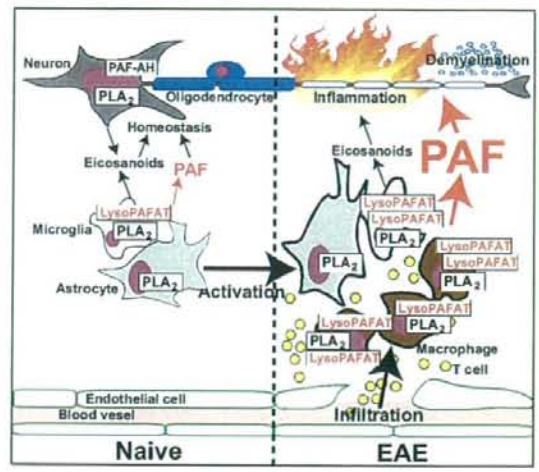

FIGURE 9. Models for PAF production in the CNS of naive mice and EAE mice. *Left*, In the CNS of naive mice, constant levels of PAF produced by microglia and astrocytes may contributes to the maintenance of CNS homeostasis. *Right*, In the CNS of EAE mice, the blood-brain barrier has been broken and inflammatory cells, such as T cells and macrophages, have infiltrated the CNS. LysoPAFAT is induced in activated microglia. Thus, robust PAF production is probably dependent on both LysoPAFAT and group IVA $cPLA_2$ coexpressed in activated macrophages and microglia.

We have measured PAF-AH activity in SCs of naive and EAE mice (Fig. 7) and found that PAF-AH activity is unchanged during the disease course of EAE. Thus, PAF may accumulate in SCs of EAE mice independently of the PAF degradation system.

Our results show that the enzyme activities in the remodeling pathway of PAF synthesis are elevated in SCs of EAE mice due to

up-regulation of group IVA cPLA$_2$ and LysoPAFAT/LPCAT2 present in macrophages and microglia (Fig. 9). Development of LysoPAFAT inhibitors may be therapeutically beneficial for the treatment of MS.

Acknowledgments

We thank Dr. N. Fukushima (Kinki University, Osaka, Japan) for advising us on the primary culturing of neurons and K. Kuniyeda (University of Tokyo, Tokyo, Japan) for valuable suggestions.

Disclosures

The authors have no financial conflict of interest.

References

1. Ishii, S., and T. Shimizu. 2000. Platelet-activating factor (PAF) receptor and genetically engineered PAF receptor mutant mice. *Prog. Lipid Res.* 39: 41–82.
2. Snyder, F. 1995. Platelet-activating factor: the biosynthetic and catabolic enzymes. *Biochem. J.* 305: 689–705.
3. Shindou, H., S. Ishii, N. Uozumi, and T. Shimizu. 2000. Roles of cytosolic phospholipase A$_2$ and platelet-activating factor receptor in the Ca-induced biosynthesis of PAF. *Biochem. Biophys. Res. Commun.* 271: 812–817.
4. Shindou, H., S. Ishii, M. Yamamoto, K. Takeda, S. Akira, and T. Shimizu. 2005. Priming effect of lipopolysaccharide on acetyl-coenzyme A:lyso-platelet-activating factor acetyltransferase is MyD88 and TRIF independent. *J. Immunol.* 175: 1177–1183.
5. Owen, J. S., P. R. Baker, J. T. O'Flaherty, M. J. Thomas, M. P. Samuel, R. E. Wooten, and R. L. Wykle. 2005. Stress-induced platelet-activating factor synthesis in human neutrophils. *Biochim. Biophys. Acta* 1733: 120–129.
6. Honda, Z., M. Nakamura, I. Miki, M. Minami, T. Watanabe, Y. Seyama, H. Okado, H. Toh, K. Ito, T. Miyamoto, and T. Shimizu. 1991. Cloning by functional expression of platelet-activating factor receptor from guinea-pig lung. *Nature* 349: 342–346.
7. Arai, H., H. Koizumi, J. Aoki, and K. Inoue. 2002. Platelet-activating factor acetylhydrolase (PAF-AH). *J. Biochem.* 131: 635–640.
8. Kudo, I., and M. Murakami. 2002. Phospholipase A$_2$ enzymes. *Prostaglandins Other Lipid Mediat.* 68–69: 3–58.
9. Kita, Y., T. Ohto, N. Uozumi, and T. Shimizu. 2006. Biochemical properties and pathophysiological roles of cytosolic phospholipase A2s. *Biochim. Biophys. Acta* 1761: 1317–1322.
10. Funk, C. D. 2001. Prostaglandins and leukotrienes: advances in eicosanoid biology. *Science* 294: 1871–1875.
11. Uozumi, N., K. Kume, T. Nagase, N. Nakatani, S. Ishii, F. Tashiro, Y. Komagata, K. Maki, K. Ikuta, Y. Ouchi, et al. 1997. Role of cytosolic phospholipase A2 in allergic response and parturition. *Nature* 390: 618–622.
12. Shindou, H., D. Hishikawa, H. Nakanishi, T. Harayama, S. Ishii, R. Taguchi, and T. Shimizu. 2007. A single enzyme catalyzes both platelet-activating factor production and membrane biogenesis of inflammatory cells: cloning and characterization of acetyl-CoA:LYSO-PAF acetyltransferase. *J. Biol. Chem.* 282: 6532–6539.
13. Pedotti, R., J. J. De Voss, L. Steinman, and S. J. Galli. 2003. Involvement of both "allergic" and "autoimmune" mechanisms in EAE, MS and other autoimmune diseases. *Trends Immunol.* 24: 479–484.
14. Steinman, L., and S. S. Zamvil. 2006. How to successfully apply animal studies in experimental allergic encephalomyelitis to research on multiple sclerosis. *Ann. Neurol.* 60: 12–21.
15. Howat, D. W., N. Chand, P. Braquet, and D. A. Willoughby. 1989. An investigation into the possible involvement of platelet activating factor in experimental allergic encephalomyelitis in rats. *Agents Actions* 27: 473–476.
16. Kihara, Y., S. Ishii, Y. Kita, A. Toda, A. Shimada, and T. Shimizu. 2005. Dual phase regulation of experimental allergic encephalomyelitis by platelet-activating factor. *J. Exp. Med.* 202: 853–863.
17. Marusic, S., M. W. Leach, J. W. Pelker, M. L. Azoitei, N. Uozumi, J. Cui, M. W. Shen, C. M. DeClercq, J. S. Miyashiro, B. A. Carito, et al. 2005. Cytosolic phospholipase A2 α-deficient mice are resistant to experimental autoimmune encephalomyelitis. *J. Exp. Med.* 202: 841–851.
18. Callea, L., M. Arese, A. Orlandini, C. Bargnani, A. Priori, and F. Bussolino. 1999. Platelet activating factor is elevated in cerebral spinal fluid and plasma of patients with relapsing-remitting multiple sclerosis. *J. Neuroimmunol.* 94: 212–221.
19. Lock, C., G. Hermans, R. Pedotti, A. Brendolan, E. Schadt, H. Garren, A. Langer-Gould, S. Strober, B. Cannella, J. Allard, et al. 2002. Gene-microarray analysis of multiple sclerosis lesions yields new targets validated in autoimmune encephalomyelitis. *Nat. Med.* 8: 500–508.
20. Pedotti, R., J. J. DeVoss, S. Youssef, D. Mitchell, J. Wedemeyer, R. Madanat, H. Garren, P. Fontoura, M. Tsai, S. J. Galli, et al. 2003. Multiple elements of the allergic arm of the immune response modulate autoimmune demyelination. *Proc. Natl. Acad. Sci. USA* 100: 1867–1872.
21. Kita, Y., T. Takahashi, N. Uozumi, L. Nallan, M. H. Gelb, and T. Shimizu. 2005. Pathway-oriented profiling of lipid mediators in macrophages. *Biochem. Biophys. Res. Commun.* 330: 898–906.
22. Kita, Y., T. Takahashi, N. Uozumi, and T. Shimizu. 2005. A multiplex quantitation method for eicosanoids and platelet-activating factor using column-switching reversed-phase liquid chromatography-tandem mass spectrometry. *Anal. Biochem.* 342: 134–143.
23. Nakanishi, H., H. Shindou, D. Hishikawa, T. Harayama, R. Ogasawara, A. Suwabe, R. Taguchi, and T. Shimizu. 2006. Cloning and characterization of mouse lung-type acyl-CoA:lysophosphatidylcholine acyltransferase 1 (LPCAT1): expression in alveolar type II cells and possible involvement in surfactant production. *J. Biol. Chem.* 281: 20140–20147.
24. Ohto, T., N. Uozumi, T. Hirabayashi, and T. Shimizu. 2005. Identification of novel cytosolic phospholipase A$_2$s, murine cPLA$_2$δ, ε, and ζ, which form a gene cluster with cPLA$_2$β. *J. Biol. Chem.* 280: 24576–24583.
25. Kume, K., I. Waga, and T. Shimizu. 1997. Microplate chromatography assay for acetyl-CoA: lysoplatelet-activating factor acetyltransferase. *Anal. Biochem.* 246: 118–122.
26. Hattori, K., M. Hattori, H. Adachi, M. Tsujimoto, H. Arai, and K. Inoue. 1995. Purification and characterization of platelet-activating factor acetylhydrolase II from bovine liver cytosol. *J. Biol. Chem.* 270: 22308–22313.
27. Ohshima, N., S. Ishii, T. Izumi, and T. Shimizu. 2002. Receptor-dependent metabolism of platelet-activating factor in murine macrophages. *J. Biol. Chem.* 277: 9722–9727.
28. Mori, M., M. Aihara, K. Kume, M. Hamanoue, S. Kohsaka, and T. Shimizu. 1996. Predominant expression of platelet-activating factor receptor in the rat brain microglia. *J. Neurosci.* 16: 3590–3600.
29. Aihara, M., S. Ishii, K. Kume, and T. Shimizu. 2000. Interaction between neurone and microglia mediated by platelet-activating factor. *Genes Cells* 5: 397–406.
30. Tabuchi, S., K. Kume, M. Aihara, and T. Shimizu. 2000. Expression of lysophosphatidic acid receptor in rat astrocytes: mitogenic effect and expression of neurotrophic genes. *Neurochem. Res.* 25: 573–582.
31. Lucas, K. K., C. I. Svensson, X. Y. Hua, T. L. Yaksh, and E. A. Dennis. 2005. Spinal phospholipase A2 in inflammatory hyperalgesia: role of group IVA cPLA2. *Br. J. Pharmacol.* 144: 940–952.
32. Svensson, C. I., K. K. Lucas, X. Y. Hua, H. C. Powell, E. A. Dennis, and T. L. Yaksh. 2005. Spinal phospholipase A$_2$ in inflammatory hyperalgesia: role of the small, secretory phospholipase A$_2$. *Neuroscience* 133: 543–553.
33. Murakami, M., and I. Kudo. 2002. Phospholipase A$_2$. *J. Biochem.* 131: 285–292.
34. Kalyvas, A., and S. David. 2004. Cytosolic phospholipase A$_2$ plays a key role in the pathogenesis of multiple sclerosis-like disease. *Neuron* 41: 323–335.
35. Lucas, K. K., and E. A. Dennis. 2005. Distinguishing phospholipase A$_2$ types in biological samples by employing group-specific assays in the presence of inhibitors. *Prostaglandins Other Lipid Mediat.* 77: 235–248.
36. Pickard, R. T., B. A. Strifler, R. M. Kramer, and J. D. Sharp. 1999. Molecular cloning of two new human paralogs of 85-kDa cytosolic phospholipase A$_2$. *J. Biol. Chem.* 274: 8823–8831.
37. Song, C., X. J. Chang, K. M. Bean, M. S. Proia, J. L. Knopf, and R. W. Kriz. 1999. Molecular characterization of cytosolic phospholipase A$_2$-β. *J. Biol. Chem.* 274: 17063–17067.
38. Cunningham, T. J., L. Yao, M. Oetinger, L. Cort, E. P. Blankenhorn, and J. I. Greenstein. 2006. Secreted phospholipase A$_2$ activity in experimental autoimmune encephalomyelitis and multiple sclerosis. *J. Neuroinflammation* 3: 26.
39. Bematchez, P. N., M. V. Winstead, E. A. Dennis, and M. G. Sirois. 2001. VEGF stimulation of endothelial cell PAF synthesis is mediated by group V 14 kDa secretory phospholipase A$_2$. *Br. J. Pharmacol.* 134: 197–205.
40. Benveniste, E. N. 1997. Role of macrophages/microglia in multiple sclerosis and experimental allergic encephalomyelitis. *J. Mol. Med.* 75: 165–173.
41. Bannerman, P., A. Hahn, A. Soulika, V. Gallo, and D. Pleasure. 2007. Astrogliosis in EAE spinal cord: derivation from radial glia, and relationships to oligodendroglia. *Glia* 55: 57–64.
42. Garcia, M. C., C. Garcia, M. A. Gijon, S. Fernandez-Gallardo, F. Mollinedo, and M. Sanchez Crespo. 1991. Metabolism of platelet-activating factor in human haematopoietic cell lines: differences between myeloid and lymphoid cells. *Biochem. J.* 273: 573–578.